Ultrafast Dynamics in Cluster Systems

T. E. Dermota, Q. Zhong,† and A. W. Castleman, Jr.*

Departments of Chemistry and Physics, The Pennsylvania State University, University Park, Pennsylvania 16802

Received August 14, 2003

Contents

1. Introduction

The vast majority of chemical reactions of practical interest take place in the condensed phase, but an understanding of the details of reaction dynamics has emerged largely from investigations in the isolated gas phase. Ascertaining the influence that solvation has on the dynamics of chemical reactions[1−8] is one of the scientifically challenging problems in the field of chemical physics. There is particular interest in elucidating details of the difference between the behavior and reactivity of ionic and neutral species in the gaseous compared to the condensed phase as a means of applying the level of understanding obtainable for gas-phase species to the systems of practical importance in condensed-phase chemistry. Studies of clusters at selectively increased degrees of aggregation offer the opportunity to explore the changes in molecular properties that are brought on by solvation. In the context of photochemistry, studies of selected excitation or ionization of selected chromophores within clusters and of the "ensuing solvation" by the cluster molecules shed light to the understanding of excitation processes in the bulk condensed state.[9−25] Studies performed at varying degrees of solvation provide new insights into the influence of solvation on the course of both ion−molecule and neutral reactions and of matter of restricted size. In terms of basic knowledge, the results of studies of the interaction of ions and molecules provide information on the forces involved, and gas-phase studies of interactions within a cluster can contribute to knowledge about the structure and bonding of complexes having analogies to those existing in solutions.

The most widely used techniques to quantify the size-dependent properties of large clusters involve ionization accompanied by subsequent mass spectrometric detection. However, the ionization step ultimately involves relaxation about the newly formed charge, with concomitant evaporative dissociation and sometimes other chemical reactions taking place. In addition to providing details on the energetics of interactions, studies of cluster ions yield information on basic mechanisms of ion reactions within the cluster (termed an intracluster reaction, sometimes distinguished as an ion−molecule half-reaction). The entire course of a chemical reaction following either a photophysical or ionizing event depends on the mechanisms of energy transfer and dissipation away from the primary site of absorption. Neighboring solvent or solute molecules can influence this by collisional deactivation (removal of energy), through effects in which dissociating molecules are kept in relatively close proximity for comparatively long periods of time due to the presence of the solvent,

* To whom correspondence should be addressed. E-mail: awc@psu.edu.
† Chemistry Division, Code 6111, Naval Research Laboratory, Washington, D.C. 20375.

10.1021/cr020665e CCC: $48.50 © 2004 American Chemical Society
Published on Web 03/25/2004

Troy E. Dermota was born in York, PA in 1970. He received his B.S. degree in chemistry from East Stroudsburg University in 1999. He is currently a fifth-year graduate student in the laboratory of A. W. Castleman, Jr., at Penn State University. He is participating in ongoing research which investigates the influence of solvent molecules on the ultrafast dynamics of ion-pair formation in acid systems and the photochemistry of atmospherically relevant molecules.

Qun Zhong received her elemental education while growing up in Xi'an, China. She earned her B.S. degree in applied chemistry from Peking University and received her Ph.D. degree from Penn State University in 1999 for work on reaction dynamics of clusters with Professor Castleman. She then spent one year as an Alexander von Humboldt postdoctoral fellow in the laboratory of Professor Martin Wolf in Fritz-Haber-Institute in Berlin, Germany, and two years as a National Research Council associate in the laboratory of Dr. Jeff Owrutsky in Naval Research Laboratory.

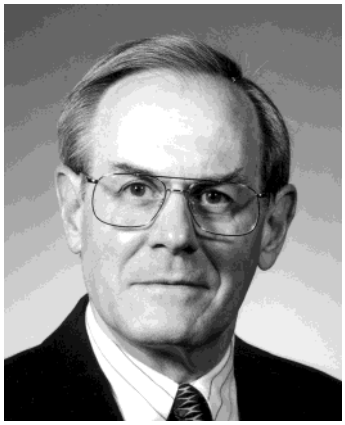

A. Welford Castleman, Jr., is holder of the Eberly Distinguished Chair of Science and Evan Pugh Professor, Departments of Chemistry and Physics, at the Pennsylvania State University. He received his undergraduate degree at R.P.I and his Ph.D. degree at the Polytechnic Institute of Brooklyn (now the Polytechnic University). He has been a group leader at the Brookhaven National Laboratory and on the faculty of the University of Colorado, Boulder. Since 1996 he has been the Editor-in-Chief for a book series devoted to *Cluster Science*/Springer Verlag. He served as a Senior Editor of the *Journal of Physical Chemistry* for 10 years and serves on the Editorial Board of a number of other scientific journals. He is a member of the National Academy of Sciences and the American Academy of Arts and Sciences. He has had a long-standing interest in the properties and dynamics of clusters and cluster ions, with application to understanding the molecular details of solvation phenomena and the behavior of matter of nanoscale dimensions.

and in other ways where the solvent influences the energetics of the reaction coordinate. Through the use of supersonic molecular beams, it is now possible to produce and tailor the composition of virtually any complex system of interest.[1−3,26,27] Utilizing these methods, coupled with femtosecond laser spectroscopy, one can selectively solvate a given chromophore (site of photon absorption/site of ionization) and investigate changes between the gas and condensed phase by selectively shifting the degree of solvent aggregation, i.e., the number of solvent molecules attached to or bound about the site of absorption of the electromagnetic radiation.

The study of cluster dynamics by employing time-resolved spectroscopy is a comparatively new subject of inquiry. Its potential has been brought to fruition through recent developments in picosecond and especially femtosecond laser pump−probe techniques.[27−30] By exploiting advances made in generating laser pulses of subpicosecond duration, the field of femtochemistry was born. Through the pioneering and innovative concepts of the Zewail group[31,32] in implementing the pump−probe technique, many breakthroughs in this emerging field already have been witnessed over the past decade. Time scales for vibrational motion that lead to bond reorganization are typically subpicosecond, and with the time resolution and coherence provided by femtosecond laser pulses, real time observation of chemical reactions, as they proceed along the reaction path from reactants to products, is made possible by employing the pump−probe technique.

This review surveys and attempts to put into perspective some of the advances that have emerged from investigations of cluster systems using femtosecond pump−probe spectroscopy. Our focus is first directed toward several characteristic mechanisms, namely, ones involving dissolution of acids and salts, photoinduced electron transfer, and excited-state charge transfer including hydrogen and single and double proton transfer. Continuing with van der Waals and hydrogen-bonded systems, some interesting experiments where cluster solvation was found to influence the coupling and transitions between electronic excited states are summarized. Next, the role of caging dynamics is discussed; here attention is given to both neutral and anionic cluster systems. Then metal cluster systems are discussed, first with a consideration of pure metal clusters. The discussion of metal-containing systems continues with an overview of recent findings on the excitation/electronic dynamics for the case of a unique semiconductor cluster system comprised of early transition metals bound to carbon in a specific composition ratio, namely, 8:12. Study of the dynamics of these clusters, termed metallocarbohedrenes, or Met-Cars for short, allows insight into electronic relaxation into elec-

tronic bands and further related understanding of how energy dissipation takes place that can lead to the phenomenon of thermionic emission in certain cluster systems. This review is concluded with a review of the phenomenon of Coulomb explosion, which was observed to occur during the course of studies of cluster dynamics using intense femtosecond laser pulses. We discuss some of the initial findings in this area including the computational models that have been applied to the Coulomb explosion process and some experimental methods that have been developed as a means of making use of the phenomenon for the study of clusters and other systems.

2. Dynamics of Acid and Salt Dissolution

2.1. Overview

The chemistry of acids is one of the most fundamental areas of solution-phase chemistry. Although thoroughly studied and understood in terms of bulk properties, the interaction between acids and their accompanying solvent on the molecular scale continues to be an area of intense scientific study driven by both scientific curiosity and practical importance. As evidenced by two recent *Science* Perspectives[33,34] on the subject, the dissolution of acids in water clusters has proven to be an effective means of studying acid−solvent interactions on the molecular level.

2.2. Excited-State Dissolution of HBr

A recent investigation of the dynamics of HBr dissolution in mixed clusters with water[35,36] is of particular interest considering the context of this article. Clusters were formed by expansion of HBr molecules diluted in Ar backing gas. The resulting $(HBr)_m$ clusters then interacted with a continuous flow of water vapor, which resulted in the replacement of HBr molecules from the cluster by the concomitant incorporation of water molecules. This technique ensured that the HBr molecules remaining were within the solvent cluster rather than attached to the outside. The clusters were then pumped into the bound Rydberg C state of molecular HBr by two photons from a 271 nm laser pulse. This excitation left the HBr molecule in a bound excited state with insufficient energy to undergo the transition to the V valence state, where the ion-pair is formed (Figure 1), which has been found to occur with excitation wavelengths in the area of 256 nm.[37] However, when the HBr chromophore is in a cluster, the energy of the V state is believed to be lowered, allowing the transition from the C state to the V state, thus enabling ion-pair formation. Probing the excited-state population, by multiphoton ionization, as a function of time produces pump−probe transients that contain temporal information about the ion-pair formation process. After an initial Gaussian-shaped response at zero delay time, the signal resulting from ionization of the $(HBr)_m(H_2O)_n$ clusters rose with increasing delay time. This rise in the signal was attributed to a reorganization of the solvent around the newly formed H^+Br^- ion-pair. In the case of the HBr

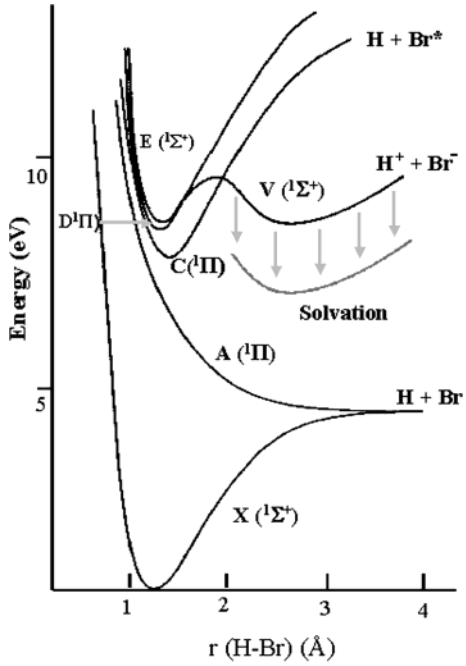

Figure 1. Potential-energy surface (PES) of HBr with downward arrows qualitatively indicating the solvation of the $V(^1\Sigma^+)$ valence state. Reprinted with permission from ref 35. Copyright 2003 American Institute of Physics.

solvated by one to four water molecules, the time constant of the rise increased from 0.5 to 2.3 ps, respectively. This increase in rise time with cluster size indicated that a significant amount of time was needed for each additional solvent molecule to reorganize around the newly formed ionic species. In addition, since detection of cluster ions required the resonant excitation of an HBr molecule, no ion signal would be detected for cluster species where the ion-pair has already formed in the ground state. Thus, the absence of any ion signal in the mass spectrum that results from an HBr molecule with more than four solvent molecules, with at least one being water, indicates that five solvent molecules are sufficient to form the H^+Br^- ion-pair in the ground state.

As was just implied, the ground-state ion-pair formation was found to occur when five solvent molecules were present, independent of whether they were HBr or water molecules as long as one water molecule was present.[35] Supporting evidence can be found in the excited-state dynamics of ion-pair formation, where the temporal behavior of, for example, the $H^+(HBr)(H_2O)_2$ and $H^+(H_2O)_3$ signals was found to be qualitatively similar with the time constant of the HBr-rich cluster being somewhat larger. These observations led to proposing that the formation of the ion-pair in HBr clusters requires the presence of a water molecule. To explain further, HBr has a coordination number of two; thus, each HBr molecule in the cluster is only interacting with two other molecules. However, when a water molecule with a coordination number of four is present, cluster structures favoring ion-pair formation can form. Additional support of the proposal that cluster structure plays a role in acid dissolution can be found in a recent discussion on the topic.[33] It was explained that computational and experimental studies of several

cluster systems have observed the onset of a three-dimensional cluster structure with a total number of molecules reaching six, while two-dimensional structures prevail in smaller clusters. It was also noted that acid dissolution appears to occur upon formation of the three-dimensional structure. Further study of HBr contained in clusters of solvents other than water should help to elucidate the influence of solvent identity and coordination number on the ion-pair formation process. In addition, the study of other acids would be very fruitful to determine how the acid strength influences ion-pair formation.

2.3. NaI Dissolution

Related studies of the cluster solvation of NaI have also been reported.[38,39] A comprehensive review of the spectroscopic, dynamics, and computational work on the solvation and ion-pair formation of NaI solvated in water, ammonia, and acetonitrile clusters has been published;[38] a discussion of the outcome of the dynamics studies on NaI solvation by water and ammonia is presented here.[39,40]

In the cluster dynamics experiments, the clusters were formed by pulsed valve expansion of the solvent vapor seeded in a backing gas, which then interacted with NaI vapor produced from an oven source. The resulting mixed clusters were then excited to the dissociative $\tilde{A}$ state of NaI by one photon of either 245 nm for $NaI(H_2O)_n$ clusters or 263 nm for $NaI(NH_3)_n$ clusters. The evolution of the excited-state population was probed by one- or two-photon ionization and detected by mass spectrometry. Excitation of the $\tilde{A}$ state of NaI was found to result in a rapid (~200 fs) dissociation of the molecule. The dissociation process results in the formation of a cluster-solvated sodium atom. After the initial dissociation process, the dynamics of the remaining cluster was reported to result in the evaporation of solvent molecules, a process driven by energy transferred to the cluster by the NaI dissociation. A clever scheme for determining the properties of the evaporation process was developed. By performing experiments with two different probe wavelengths and varying the clustering conditions, the likelihood of neutral excited-state and ion-state evaporation was determined along with the time scale of the neutral-state evaporation process, which was found to be about 20 ps.

Analogous to the HBr experiment, the detection of ion-state clusters depends on excitation of the $\tilde{A}$ state followed by absorption of ionization photon(s). As a result, clusters large enough to produce ground-state ion-pair formation will not be ionized or detected. Ground-state ion-pair formation did not appear to occur when water was the solvent since all cluster sizes that were expected to be produced could be ionized. It was reported that dissolution of NaI in the water clusters did not occur because the interaction between the water molecules was too strong to allow the NaI molecule to enter the cluster, thus remaining on the surface rather than being solvated. Ground-state ion-pair formation did appear to occur when ammonia was the solvent as clusters did not appear to be present with more than about seven ammonia molecules.

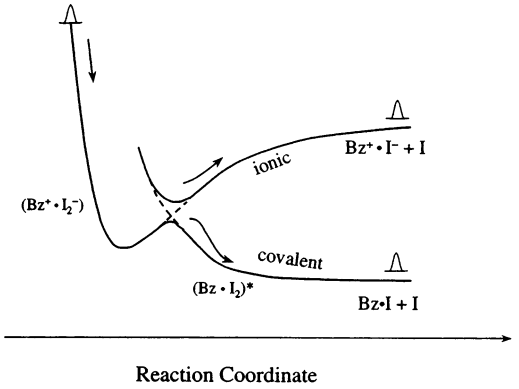

Figure 2. Schematic of the potential-energy curves of the dissociative electron-transfer reaction along the reaction coordinate in $Bz \cdot I_2$ system. Reprinted with permission from ref 50. Copyright 1996 American Institute of Physics.

Due to the fundamental chemical nature of the dissolution of ionic and acid species, the study of this process will undoubtedly continue to produce results of scientific significance.

3. Charge-Transfer Reactions

3.1. Overview

Charge-transfer reactions are of fundamental importance in a wide range of chemical and biological processes, including acid−base interactions, charge migration in DNA,[41,42] processes in photosynthetic reaction center,[43] etc., and there is a continuous and growing interest in determining the molecular details of the elementary charge-transfer steps.[44−47] However, charge-transfer processes in natural environments are quite complex, so researchers endeavor to study charge-transfer reaction in well-defined cluster systems with well-characterized optical pulses as a route to understand the elementary aspects of this process, free from complicating or competing processes found in natural environments. The intent of this section is to give an overview of some of the experimental studies of photoinduced charge-transfer reaction in gas-phase clusters, focusing on photoinduced electron transfer and excited-state proton transfer.

3.2. Photoinduced Electron Transfer

When iodine and benzene were dissolved in *n*-heptane solvent, a new UV absorption band was observed and attributed to an electronic transition from the highest occupied molecular π orbital of benzene to the lowest unoccupied molecular σ^* orbital of iodine.[48,49] In the isolated gas phase, the bimolecular complex of benzene (Bz) and iodine, $Bz \cdot I_2$, formed by supersonic expansion, was found to undergo a similar photoinduced electron-transfer process (PET); subsequent dissociation of I_2 occurs following an electron back transfer to Bz.[50] As shown schematically in Figure 2, in excited states of the $Bz \cdot I_2$ complex, the avoided crossing between the bound ionic state and the repulsive covalent state forms an upper quasibound potential well and a lower potential well with a barrier at the crossing. Upon excitation at 277 nm to the ionic potential surface (PES),

some of the $Bz^+ \cdot I^- \cdots I$ population can propagate across to the neutral PES through an electron back transfer to the Bz molecule, leading to the cleavage of the I−I bond in 0.45 ps, releasing a fast I atom. The release of the trapped I atom in Bz·I occurred in 1.4 ps, and the associated kinetic energy was lower than that for the first I atom.[50] When I_2 was replaced by ICl, only a slow I atom was released in 0.95 ps, indicating that ICl binds to Bz through the I atom, Bz·ICl.[51]

When the $Bz \cdot I_2$ complex was solvated in Bz clusters, the bimodal release of the two I atoms remained but at a slower rate due to cluster caging dynamics.[50] Theoretical calculations[52] indicate that the two-step dissociation may be attributable to the asymmetric structure of the $(Bz)_n I_2$ clusters, with the iodine molecule protruding out of the benzene cluster, leaving one of the I atoms more strongly solvated than the other. Following the I−I bond rupture, the outer I atom leaves the cluster quickly, dragging some Bz molecules with it. This free I fragment was detected in the subpicosecond to picosecond time scale, depending on the degree of solvation. The inner I atom was caged by the remaining Bz cluster, and its escape took longer than a few tens of picoseconds.

The ease with which iodine accepts an electron from a photoexcited donor molecule makes it an ideal electron-acceptor molecule to study this PET and subsequent dissociation dynamics. In addition to Bz, PET in bimolecular complexes of iodine with other electron donors such as acetone, diethyl sulfide, dioxane, and *o*-xylene have been studied.[50,51] Results indicate that longer escape times correlate with stronger interaction between donor and iodine.

Electron-transfer-mediated photochemistry in hydrocarbon$-O_2$ complexes also have attracted some attention due to its potential impact on the photooxidation cycles in polluted urban areas.[53−55] Similar to the $Bz-I_2$ complex, excitation of alkene$-O_2$ and $Bz-O_2$ at 226 nm lead to PET, followed by an electron back transfer, leaving O_2 in its highly vibrational excited state, which subsequently dissociates.[53,54] To the best of our knowledge, no time-resolved studies have been performed on these systems, which could offer more insight into the reaction dynamics.

3.3. Excited-State Proton Transfer

Many molecules such as aromatic enols become acidic upon electronic excitation. For example, the pK_a of 1-naphthol changes from 9.4 in its ground electronic state to 0.5 in its S_1 state;[47] when dissolved in basic solvents, proton transfer can occur from solute to solvent upon photoexcitation. This excited-state proton-transfer process (ESPT) was first observed when 1-naphthol was dissolved in solution, where a strong red shift of the fluorescent emission was observed and attributed to the proton-transferred naphtholate anion.[56,57] Since then, ESPT has been extensively studied in gas-phase clusters.[58−78] There are a number of good review articles on this subject,[60,61,71,72] especially regarding mixed clusters of 1-naphthol or phenol with ammonia. Here we discuss some of the highlights.

Gas-phase experiments revealed that the excited-state dynamics of aromatic enols (such as naphthol and phenol) solvated by ammonia clusters changed drastically at a threshold ammonia cluster size, n_c.[58−68,72] In the frequency domain, for clusters at $n \geq n_c$, the absorption band red shifted by hundreds of wavenumbers, laser-induced fluorescence emission red shifted by thousands of wavenumbers, and the structure of both bands changed from sharp and resolved to diffuse and structureless[73,74] (Figure 3); in the time domain, the transient lifetime of parent clusters decreased dramatically at $n \geq n_c$, and the corresponding protonated ammonia clusters appeared with a rise time that agreed with the respective decay time of the parent clusters (Figure 4).[58−68,72] The observed drastic changes in dynamics and spectroscopy at a specific threshold cluster size were attributed to the onset of ESPT. ESPT threshold was found to depend on the acidity of the excited chromophore, the proton affinity of the solvent, and the corresponding solvent structure. A relatively large amount of energy is needed to free a proton from the excited chromophore as the resulting proton transferred ion-pair is unstable compared to the original covalent structure. Solvation of the proton with a high proton affinity solvent can enhance the stability of the ion-pair significantly. Studies show that for strong base solvents, such as the nitrogen bases ammonia and piperidine,[61,72] ESPT occurs in the picosecond time scale with a clear threshold that becomes smaller for systems accompanied by stronger bases. In these clusters, ESPT may occur through an adiabatic channel where the chromophore and the solvent are strongly coupled such that ESPT proceeds on a single electronic surface, which has a low barrier for proton transfer. For weak base solvents, such as the oxygen bases water and methanol, ESPT was found to occur at much larger cluster sizes with no distinct threshold and at a much slower rate that decreases with cluster sizes, in contrast to clusters

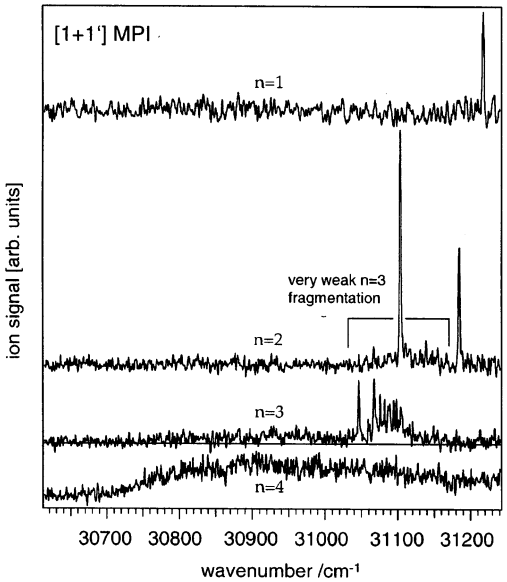

Figure 3. The 1+1′ multiphoton ionization spectra of 1-$NpOH(NH_3)_n$ clusters. For $n = 1-3$, structured spectra were obtained, however, the spectrum of $n = 4$ became broad, unstructured, and red-shifted, indicating excited-state proton transfer. Reprinted with permission from ref 72. Copyright 2002 Elsevier.

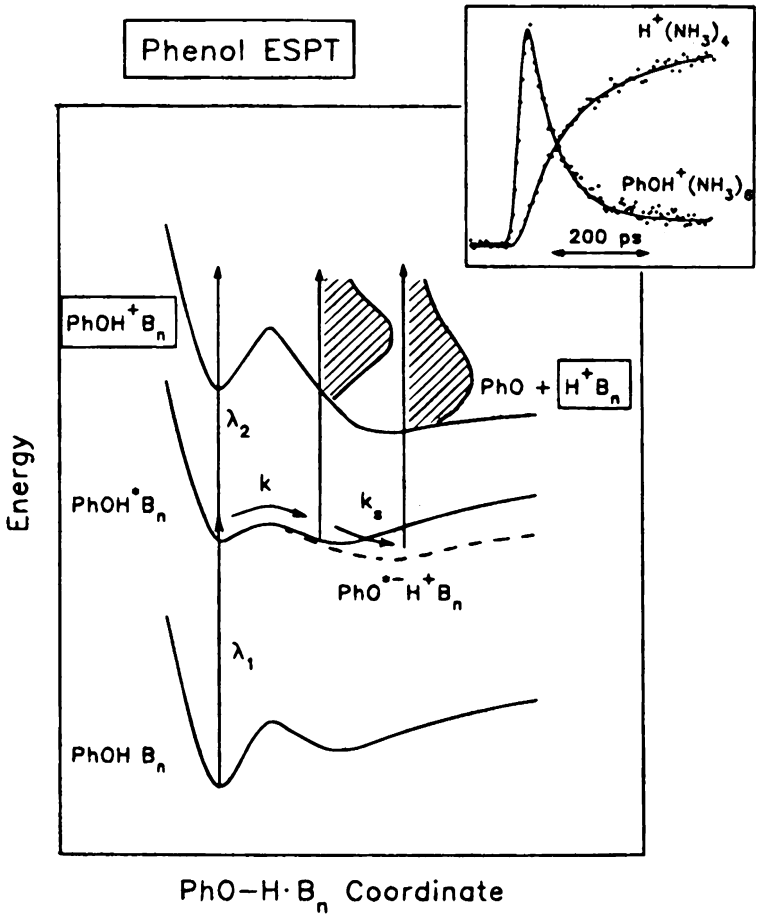

Figure 4. Schematic energy diagram for $PhOH(NH_3)_n$ (NH_3 is represented by B). The pump (λ_1) and probe (λ_2) are denoted by the vertical arrows. The excited-state proton transfer and solvent reorganization rate constants are given by k and k_s, respectively. Approximate photoelectron band shapes are shown by the shaded areas. The insert shows the ion signals for reactant and product clusters. Reprinted with permission from ref 60. Copyright 1995 American Chemical Society.

involving nitrogen bases. ESPT in these systems may be better described as a nonadiabatic process, where the coupling between the chromophore and the solvent is weak and the electronic state of the chromophore remains largely unchanged. In these cases ESPT occurs due to solvent reorganization around the electronically excited chromophore and subsequent relaxation.[72]

However, this ESPT picture for the S_1 state of enol ammonia clusters has been challenged, and hydrogen-atom transfer (or synchronized proton and electron transfer) was proposed to account for the excited-state dissociation dynamics, especially in small clusters.[69−71] The excited-state hydrogen-atom transfer (ESHT) was thought to occur via system crossing to a higher lying singlet state ($^1\pi\sigma^* \leftarrow {}^1\pi\pi^*$) where photoexcited enol chromophore donates a hydrogen atom from the OH group to the solvating cluster. Studies by Jouvet and co-workers[71] show that the ESHT rate was sensitive to the vibrational excitation, where excitation of the intermolecular stretching mode seems to accelerate the H-atom transfer.

As we know, for femtosecond cluster studies, selective excitation of a specific cluster size is not possible due to the inherent laser bandwidth. Hence, data analysis could be obscured by larger clusters feeding down to smaller ones due to evaporative cooling in the neutral and/or ionic states. In addition, ground-state proton transfer, which can occur when the solvent cluster reaches a specific size,[79] could add one more degree of complexity. On the basis of these considerations, Jouvet and co-workers[69−71] explained the observed dissociation dynamics of mixed enol ammonia clusters, including the threshold change in frequency and time domains, by a combination of ESHT, ground-state proton transfer, and possible evaporation process in neutral and ionic clusters without invoking ESPT. Theoretical studies[76−78] have shown that ESPT and ESHT processes are energetically possible beyond a specific cluster size. In light of these findings, more studies and further analysis of earlier data are called for to further understand the excitation and dissociation mechanisms of these systems.

ESHT in clusters is not a rare phenomena; it has been observed in pure ammonia clusters,[80−83] in mixed methanol water clusters,[84] and in mixed indole ammonia clusters.[85−87] For the excited Ã state of pure ammonia clusters, ESHT occurs within a few hundreds of femtoseconds,[83] whereas for the *C* state of ammonia clusters, both ESPT and ESHT channels were found to take place at 85−135 and 300−1500 fs, respectively.[80] The larger dependence of ESHT on cluster size can be accounted for by the role the out of plane "umbrella" bend plays in the dissociation process. The "umbrella" bend, which moves along the hydrogen-atom transfer coordinate but perpendicular to the proton-transfer coordinate, is highly excited

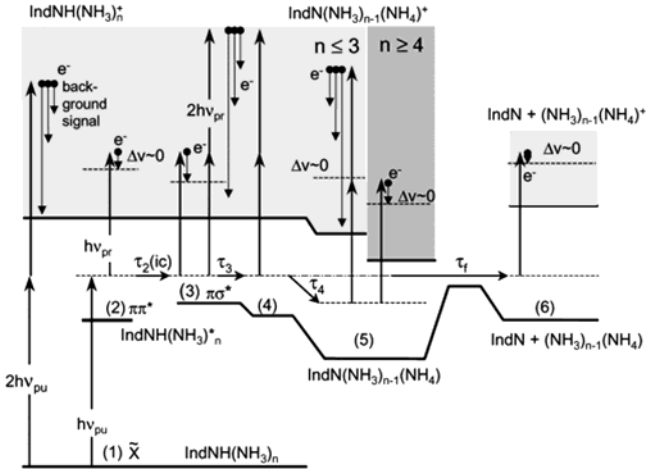

Figure 5. Proposed kinetic model and energetics for the excitation and ionization of small indole ammonia clusters. τ_2 = time constant for internal conversion, $\pi\pi^* \rightarrow \pi\sigma^*$; τ_3 = time constant for H transfer on the $\pi\sigma^*$ surface; τ_4 = relaxation time to equilibrium state $IndN(NH_3)_{n-1}NH_4$; τ_f = product formation time. Reprinted with permission from ref 88. Copyright 2003 Elsevier.

when ammonia is excited to the *C* state. The quenching rate of the bending excitation should increase with cluster size, and therefore, ESHT should display a higher dependence on degrees of solvation as observed.

Excitation of a CH_3OH molecule to its 3p Rydberg state leads to a loss of a hydrogen atom via internal conversion to the 3s Rydberg state, which dissociates along the O−H coordinate.[84] In the presence of neat methanol clusters, the dissociating H atom can be captured by the clusters, resulting in ESHT on the time scale of ~400 fs. When one of the methanol molecules in the cluster was replaced by a water molecule, a long decay component on the time scale of several tens of picoseconds appeared in addition to the subpicosecond ESHT dynamics, which was attributed to the lifetime of the $(CH_3OH)_mH\cdot(H_2O)^*$ transient. Experiments with H-methanol and D_2O provided evidence that H-atom transfer originates from the methanol chromophore. In water-rich $(CH_3OH)_m\cdot(H_2O)_{n=2\sim4}$ clusters, the ESHT rate decreases from 570 to 760 fs while the long time decay component experiences a steep shortening from 13.7 ps to approximately 3 ps as *n* increases. These results suggest that the $H_3O(H_2O)_n$ cluster becomes less stable as *n* increases.

ESHT in mixed indole ammonia clusters,[85−88] $[IndNH(NH_3)_n]$, was thought to occur similarly as proposed for mixed enol ammonia clusters. As shown schematically in Figure 5, upon excitation to the S_1 state ($\pi\pi^*$) at 263 nm, internal conversion to a high-lying $\pi\sigma^*$ state occurred in about 150 fs (for $n = 1-6$), followed by hydrogen-atom transfer on the $\pi\sigma^*$ surface on the time scale of 700−800 fs for $n = 1-3$. The hydrogen-transferred cluster transient undergoes solvation reorganization within 100 ps. For large clusters ($n > 4$), the H-atom transfer process was not observed probably due to Franck−Condon reasons, while a structural rearrangement mechanism after the H transfer on a time scale of 10 ps for $n = 4$ and subpicosecond for $n = 5-6$ was clearly recognized. During this structural rearrangement, some clusters dissociate on a time scale of 70−160 ps via a weak channel, leading to hydrogenated ammonia clusters.

In addition to the studies of the hydrogen transfer between indole and ammonia, $IndNH(H_2O)_n$ clusters have been studied[89] using a similar experimental technique. However, when water was the solvent, evidence of hydrogen transfer was not observed as it was in the ammonia case.

3.4. Excited-State Double Proton Transfer

Interactions between hydrogen-bonded nucleobases of DNA and RNA are responsible for the storage and transfer of biological information. These interactions are thought to be in terms of the keto−amine tautomers, the dominant forms of the base pairs in duplex DNA. However, radiation-induced mutation may occur through a double proton transfer, leading to an enol−imine tautomer.[90,91] To understand the fundamental aspects of the multiple proton-transfer process in complex molecular networks, 7-azaindole dimer and its derivatives, which mimic the base pairs, were chosen as model systems due to their reduced complexity.[92−102]

The excited-state double proton transfer (ESDPT) of the 7-azaindole dimer was first observed on its S_1 state by Kasha et al. in solution[94] and has since been studied extensively in the gas phase.[92,93,95−100] The first time-resolved measurements of the 7-azaindole dimer in the gas phase were performed by the Zewail group, where two distinct steps for the double proton transfer were observed in 650 fs and 3.3 ps, respectively, for the ground vibrational state and become shorter with higher vibrational excitation.[99] The Castleman group confirmed the stepwise double proton-transfer mechanism utilizing a Coulomb explosion (CE) imaging technique described in the section on Coulomb explosion.[92,93]

The 7-azaindole dimer has two isomers, whose formation depends on the stagnation pressure employed in the supersonic expansion. Due to the structural difference, one isomer undergoes normal ESDPT while the other does not. These isomers are termed the reactive and nonreactive dimers, respectively.[96] The existence of reactive and nonreactive dimers was confirmed by time-resolved measurements in the Castleman lab.[103] The reactive dimer transient displays a biexponential decay with similar time constants to those observed by the Zewail group;[99] the nonreactive dimer transient was stable within the observation window of the experiments, which indicated that ESDPT had not occurred. Of particular interest was that the nonreactive dimer became reactive when solvated with water molecule(s). Figure 6 shows the nonreactive dimer transients with 0, 1, and 2 solvated water molecules. Even with only one solvating water molecule, the nonreactive dimer displayed a biexponential decay on the same time scale as those of the reactive dimer. Most strikingly, subsequent solvation beyond one water molecule had little effect on the proton transfer until a dramatic change occurred at four waters, where only a single proton-transfer step was observed for five or more water molecules (Table 1). These results

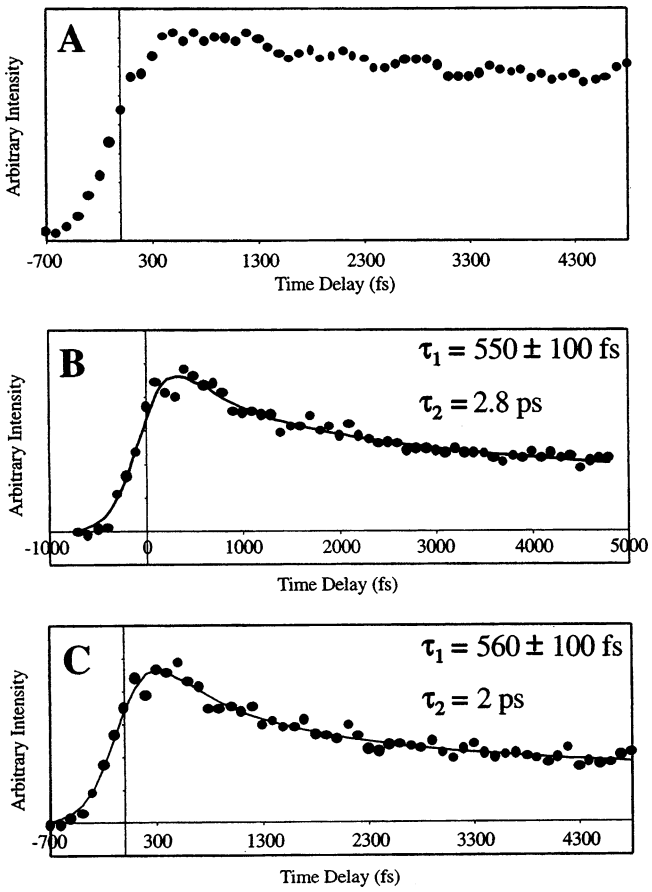

Figure 6. Water solvation effect on ESDPT of 7-azindole dimer. (A) Pump−probe transient of the nonreactive dimer (stagnation pressure, 1200 Torr); (B) Pump−probe transient of the nonreactive dimer with one water clustered to it. It can be seen here that an attached water molecule actually facilitates the occurrence of the proton transfer in an otherwise nonreactive species. (C) Pump−probe transient of the nonreactive dimer with two waters clustered to it. The second step of the proton transfer can be seen to occur even more quickly with two waters present. Reprinted with permission from ref 103. Copyright 1999 National Academy of Sciences.

Table 1. Proton-Transfer Times for Solvated 7-Azaindole Dimers

no. of waters	first transfer, fs	second transfer, fs	transfer time, fs
1	550 ± 100	2800	
2	565 ± 100	2000	
3	560 ± 100	2000	
4	*a*	*a*	
5			1800
6			1600
7			1300
8			1100
9			1000

[a] No definite lifetimes could be determined from the $n = 4$, which was reported to be due to a change in the cluster structure when four water solvent molecules were present. Reprinted with permission from ref 103. Copyright 1999 National Academy of Sciences.

suggest that the double proton transfer may undergo a transition from a stepwise to a concerted process upon progressive clustering. Alternatively, the 7-azaindole dimer may adopt a non-hydrogen-bonded stacked structure at higher degree of hydration,[104] and the observed single-exponential decay could result from a self-tautomerization of the excited 7-azaindole moiety via a catalytic water bridge. Further experimental and theoretical works are needed to elucidate this interesting behavior.

Unlike the 7-azaindole dimer, which has been extensively studied experimentally, investigations of ESDPT in other dimer systems have been sparse. One time-resolved study was the amino−imino ESDPT of the 2-aminopyridine (2AP)/acetic acid system in hexane, where the ESDPT was found to occur in a stepwise mechanism; though the first step proton transfer could not be resolved, the second step occurred in 5 ps.[105] There are no reports on isolated phase in these systems, and it would be valuable to investigate this system in the cluster environment and learn how the solvation affects the ESDPT process.

Though there are very few experimental studies on ESDPT in systems other than the 7-azaindole dimer, ESDPT has attracted wide interest in the theoretical community.[101,102,106,107] Of particular interest are the ab initio calculations of formamide−formamidine dimer mimicking adenine−thymine base pairs,[105] where the ESDPT was found to occur in a concerted mechanism in the isolated dimer but becomes stepwise when solvated by polar medium, in contrast to 7-azindole. It would be interesting to confirm these results by time-resolved experiments.

4. Excited-State Coupling

4.1. Overview

Following an initial photoexcitation, an electronically excited molecule can undergo a number of transitions to lower lying electronic states through various coupling mechanisms that link the quantum states of a molecule. Two such process that have been studied in cluster dynamics experiments are internal conversion between bound valence states and intersections between a bound Rydberg state and a dissociative valence state.

4.2. Internal Conversion

Internal conversion is, in basic terms, the transfer of energy from an electronic excitation to vibrational energy in a lower lying electronic level. Studying the dynamics of internal conversion in clusters thus provides two scientifically interesting pieces of information: the influence that cluster solvation has on the rate of the internal conversion process and the effect the high level of vibrational excitation, which follows internal conversion, has on the cluster. Study of the dynamics of internal conversion has been the subject of several investigations, including those of the toluene dimer,[108] the benzene dimer,[109,110] and benzene solvated in ammonia clusters.[111−112]

The newest study of internal conversion in the benzene dimer[109] was performed using the recently developed ultrafast photoelectron spectroscopy technique incorporating coincidence detection to correlate the detected electrons with concurrently generated cluster ions. This technique allows the simultaneous determination of excited-state lifetimes and the energy of the excited state through measurement of

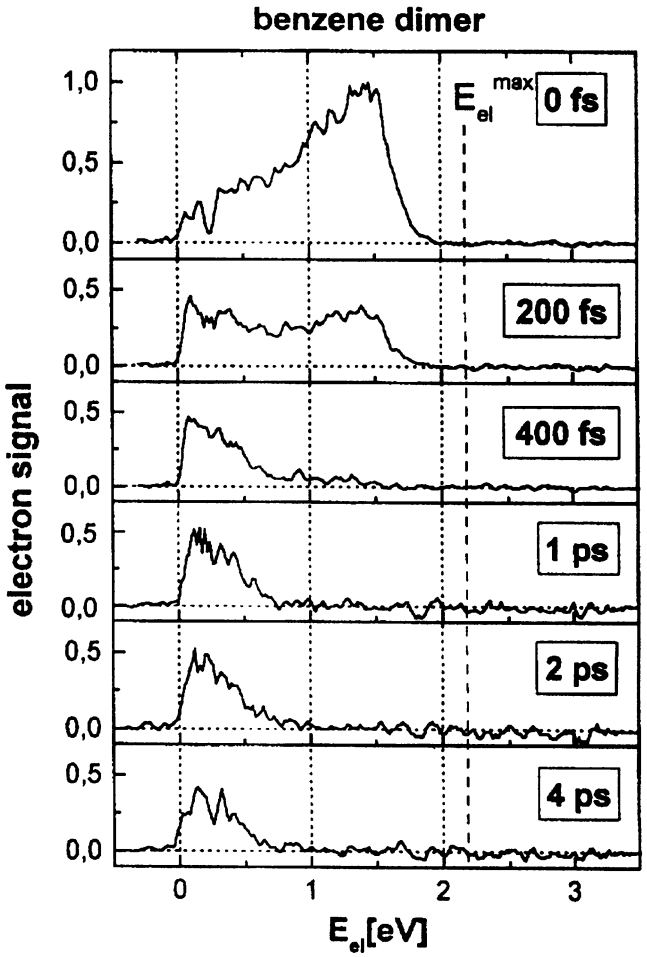

Figure 7. Femtosecond time-resolved photoelectron spectra of the benzene dimer. Note the difference in the time scale of the high-energy electrons that were detached from the S_2 state as compared to the low-energy electrons originating from the S_1 state. Reprinted with permission from ref 109. Copyright 1997 Elsevier.

the kinetic energy of photoelectrons. The reader is referred to ref 113 for experimental details. Briefly, benzene monomer and clusters were pumped to the S_2 excited state by one photon of 200 nm light. The excited-state species were then ionized by either a 400 or 267 nm photon. When the 400 nm probe was used, benzene could be ionized only while the S_2 state was populated. As a result, the ion and photoelectron signals decay rapidly with time as the excited molecule undergoes the internal conversion process from the S_2 to the S_1 and S_0 states. The S_2 state decay was found to have a time constant of 50 fs for the monomer and dimer. When the 267 nm probe was used, the excited-state species could be ionized from either the S_2 or S_1 states. From the photoelectron spectra of the 267 nm ionization (Figure 7), the lifetime of both excited states can be determined since the kinetic energy of electrons from the S_1 excited species will be lower than those from the S_2 state. In addition, the likelihood or branching ratio of the S_2 state undergoing internal conversion to the S_1 as compared to the S_0 can be determined by comparing the relative intensity of the electron signals at high and low kinetic energy. The temporal behavior of the S_1 state was found to have a growth component of about 50 fs for both the monomer and dimer, corresponding to the conversion from the S_2 state followed by 6.7 ps conversion from the S_1 to the S_0 for the monomer and greater than 100 ps for the dimer. The inhibition of internal conversion to the S_0 ground state by dimer formation, as indicated by the significant increase in the S_1 state lifetime, is substantiated by the branching ratio of the S_2 state conversion to the S_1 and S_0. The branching ratios indicate that only 1% of the S_2 state population undergoes conversion to the S_1 in the monomer, but 2.3% of the population was found to convert to the S_1 for the dimer.

Toluene and the toluene dimer[108] were also studied by the same technique used in the benzene experiment. In the toluene experiments a 202 nm pump and 269 nm probe were employed. Analysis of the time-dependent photoelectron spectra indicated that the S_2 state lifetime for the monomer and dimer was about 50 fs and that the S_1 state lifetime increased from 4.3 ps for the monomer to greater than 100 ps for the dimer, which is similar to the results observed for benzene. The most dramatic difference between benzene and toluene is that a significantly greater portion of the S_2 population undergoes internal conversion to the S_1 in toluene with 30% S_2 to S_1 conversion for the monomer and 70% for the dimer. The substantially increased probability of the S_2 to S_1 transition in toluene is thought to be due to the higher density of vibrational levels compared to benzene, thus improving the coupling between the S_2 and S_1 states.

Influences of solvation similar to those seen for the benzene and toluene dimer systems have been observed for internal conversion in benzene solvated in ammonia clusters.[111] The benzene$(NH_3)_n$ clusters were pumped to the S_2 state with a 200 nm photon and then ionized with 267 nm light allowing detection of the ions by time-of-flight mass spectrometry. Two components were observed in the pump−probe transients corresponding to the fast (40 fs) internal conversion from the S_2 to S_1 and S_0 followed by a slow component representing S_1 to S_0 conversion as before. The lifetime of the S_1 state was found to be substantially lengthened by ammonia solvation with the time constants for the S_1 state decay increasing with n for the size range studied ($n = 1-4$); values of the lifetimes ranging from 50 to 100 ps were found. The branching ratios for conversion from the S_2 state also followed the trend discussed above with the percentage of the population going into the S_1 increasing from 1.1% for benzene to 15% when the benzene molecule was solvated with four ammonia molecules. The increased branching ratio was attributed to an increase in the vibrational density of states of the benzene molecule due to a breaking of the molecules symmetry by the cluster. This interpretation is consistent with the observation that the toluene molecule and dimer have greater probabilities of conversion to the S_1 due to lower symmetry and greater density of vibrational modes.

A final interesting note which applies to all of the internal conversion systems discussed above is that evaporation of molecules from the clusters was not observed on the microsecond time scale of the mass spectrometer. This is significant because, as men-

tioned at the beginning of this section, internal conversion results in the excited molecule possessing a large amount of vibrational energy, about 2.1 eV in the case of the benzene dimer experiment, which will be retained in the cluster after ionization. This vibrational energy is significantly greater than the binding energy of the cluster; thus, the lack of evaporation indicates that the intermolecular vibrational modes do not couple strongly with the vibrational modes of the cluster.

Although the relaxation process has only tentatively been assigned as internal conversion, it seems reasonable to discuss the study of sodium[114−117] and silver[118] solvated by ammonia clusters here since a substantial influence of solvation on the electronic state relaxation time has been observed with these systems. The mixed clusters were formed by passing an ammonia cluster beam, formed by pulsed valve expansion, through an effusive beam of sodium vapor in all cases. In the earliest experiment performed on $Na(NH_3)_n$,[116] the clusters were pumped to an excited state by a 820 nm laser pulse followed by ionization with a 410 nm probe pulse. The 820 nm pump results in a single-photon excitation of the $\tilde{A}\ ^2E$ state of $Na(NH_3)$, which was found to have a lifetime on the nanosecond time scale. However, due to the solvation shift of the potential-energy surface, 820 nm light results in a two-photon excitation of an unassigned high-energy state of the $Na(NH_3)_2$ cluster. The ion signal of this cluster exhibited a decay time constant of ~30 ps, while the Na^+ ion signal was found to rise with the same time constant, indicating that the decay of the $Na(NH_3)^+$ is the result of a fragmentation of the excited cluster. A further study of $Na(NH_3)_n$[117] was performed at a range of pump wavelengths from 820 to 1690 nm. The tuning of the pump wavelength allowed excitation of the same transition for each cluster size, namely, the 3s → 3p transition of the Na atom up to $n = 15$. The lifetime of the excited-state clusters dropped from 1 ns for $n = 1$ to 1 ps for $n = 3$. The decrease in lifetime continues with increasing n until the lifetime of the largest cluster studied has a time constant on the order of 200 fs.

Similar results were observed when silver was solvated in ammonia clusters.[118] A 475 nm pump was used to excite the $X \rightarrow \tilde{A}$ of the $Ag(NH_3)_n$ with $n = 1-15$. The lifetime of the excited species was found to decrease sharply with cluster size, as seen in the solvated Na experiments, from 25 ps for the $n = 2$ cluster to 930 fs for $n = 3$. The lifetimes then decrease gradually to a time constant of 400 fs for $n = 15$.

The decay process was interpreted as being the result of internal conversion from the electronic excited state of the Na or Ag atom to the vibrational modes of the ammonia cluster. This would have to be a somewhat different form of internal conversion than the benzene and toluene systems discussed above as the proposed relaxation mechanism involves transfer of energy between the molecules of the cluster rather than within the excited-state molecule itself.

4.3. Rydberg to Valence Coupling

Continuing the discussion with a consideration of coupling between Rydberg and dissociative valence states, two systems have been studied that employed cluster solvation: methyl iodide clusters[119] and acetone solvated in acetone or water clusters.[120]

The findings of the methyl iodide cluster studies have been discussed in a previous review,[27] so only a brief discussion will be presented here. Spectroscopic results[121] and ultrafast dynamics studies[122,123] indicate that a methyl iodide molecule excited to Rydberg states will strongly couple to the dissociative $\tilde{A}$ state, resulting in a dissociation of the molecule in about 200 fs. However, the spectroscopic studies found that the coupling was weakened when clusters were present.[124] The dynamics studies of methyl iodide clusters[119] showed a slowing of the dissociation from the 10s Rydberg state by about 50 fs for clusters when compared to the monomer, which is consistent with the spectroscopic observations of decreased coupling. Caging dynamics were also observed in methyl iodide clusters, but this will be discussed in another section of the review.

Recent findings for acetone clusters and acetone clustered with water[120] also indicate that the Rydberg to valence coupling can be altered by cluster solvation. Mixed acetone−water clusters and acetone clusters were simultaneously generated by a pulse valve co-expansion of acetone and water vapor seeded in argon. The clusters were excited to the 5d Rydberg state by three 407 nm photons. Thereafter, the clusters were ionized by an 814 nm pulse followed by mass spectrometric detection. The experimental results showed that the acetone monomer exhibits a rapid decay that was observed to be shorter than the 100 fs laser pulse width. The dynamics of the acetone clusters and water-containing acetone clusters exhibited a fast, less than 100 fs, decay followed by a slow decay on the order of picoseconds. With the $(acetone)_nH^+$ clusters, a clear size-dependent trend was observed with the lifetime increasing from 0.5 to 6.3 ps for $n = 1$ to 3, respectively. Spectroscopic studies of the Rydberg states of acetone[125] have revealed that they are strongly coupled to the dissociative valence states and lower lying Rydberg states. Thus, excitation of the 5d Rydberg state is expected to result in the rapid dissociation of acetone to CH_3 and CH_3CO through Rydberg to valence coupling. This result indicates the coupling between the 5d Rydberg state and the dissociative valence state is hindered by cluster solvation, an effect which has also been observed through spectroscopic studies of acetone clusters.[126]

An explanation of the decrease in the effectiveness of Rydberg to valence coupling with clustering has been proposed for both methyl iodide[121] and acetone[126] based on spectroscopic data. The proposed process,[127] dubbed the cluster-induced potential shifts model, explains the change in coupling as follows. The bonding of a molecule in a bound Rydberg excited state is not expected to be altered significantly, relative to the ground state, since the excitation is the result of a transition between two nonbonding orbitals. Thus, the Rydberg-excited molecule is expected to be stabilized in about the same way as the ground state. On the other hand, an excitation to a dissociative state is the result of an electronic transi-

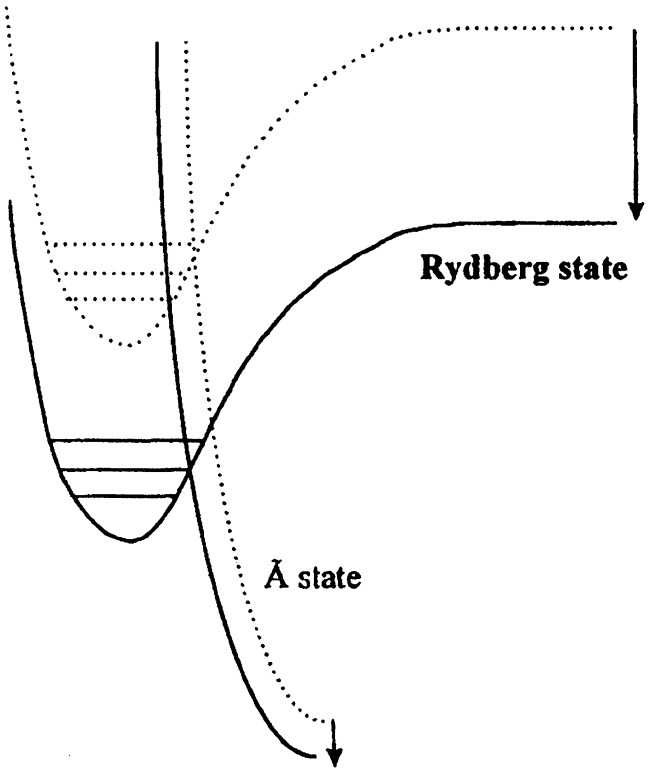

Figure 8. Graphical representation of the solvation shift of a Rydberg relative to dissociative valence state. Note that in this case a higher vibrational level in the Rydberg state would have to be populated for coupling to occur. Reprinted with permission from ref 119. Copyright 1998 American Institute of Physics.

tion from a nonbonding orbital to an antibonding orbital. This transition will significantly alter the interaction between the excited-state molecule and the solvent. Thus, as depicted in Figure 8, the dissociative state should not be shifted by solvation in the same way as the Rydberg state, resulting in a mismatch between the states that leads to a hindering of coupling to the dissociative state when clusters are present.

Results somewhat different than those discussed above were observed in the case of SO_2 clusters pumped to the C ($2^1A'$) state by two 397 nm photons followed by multiphoton ionization with a ~795 nm probe.[128] The SO_2 molecule is known to undergo predissociation from the C state to the $2^1A'$ repulsive surface, leading to the loss of an oxygen atom from the molecule. A decay in the cluster signal on the order of 0.5 ps for clusters up to three molecules was observed which was attributed to the predissociation process. An additional component was observed in the transients of the SO_2^+ and SO^+ signal and the signal of the S^+ and O^+ ion state fragments that was not present in the transients of the clusters. This additional component consisted of a ~100 fs growth preceding the decay component. It was proposed that the growth component in the monomer species was present because the excited-state SO_2 molecule within the cluster may, in some cases, evaporate from the cluster, leading to an increase in the monomer population. The evaporation mechanism was supported by an energetics argument. The two-photon pump resulted in an excitation of the C state to 0.57 eV above the crossing between the C and $2^1A'$ states. Thus, the excited-state molecule must dissipate the 0.57 eV of energy before crossing to the $2^1A'$ surface. This energy was expected to lead to the evaporation process.

An investigation of the influence of cluster solvation on two processes occurring in clusters of [tetrakis(dimethylamino)ethylere] (TDMAE) has been performed.[129] The two processes are the transition from the valence V($\pi\pi^*$) to the zwitterionic Z(π^{*2}) state through a conical intersection and the ion−molecule reaction between the $TDMAE^+$ and $(TDMAE)_n$ of the cluster following ionization. The $(TDMAE)_n$ clusters were pumped to the V($\pi\pi^*$) state by one photon of 266 nm light followed by a second laser pulse of 800 nm light to ionize the cluster. The V($\pi\pi^*$) to Z(π^{*2}) transition was found to occur in 200 fs, somewhat faster than the 300 fs transition observed for the monomer. It was also found that when the $(TDMAE)_n$ clusters were ionized by the absorption of the 266 and 800 nm laser pulses, an ion−molecule reaction occurred that resulted in the loss of 84 amu from the cluster leading to the formation of, for example, a 316 amu cluster from the 400 amu dimer. The products of the ion−molecule reaction, such as the 316 amu cluster, were found to have greater intensity when there was a time delay between the two laser pulses than when the delay between the pulses was zero, whereas the intact 400 amu dimer cation was at its greatest intensity near zero delay time. This observation indicated that the temporal evolution of the neutral cluster was influencing the occurrence of the ion−molecule reaction in the positively charged cluster. It was concluded that at short delay times the clusters were ionized into a metastable potential well with a barrier to the ion−molecule reaction, inhibiting the production of the 316 amu cluster. However, a time delay between the two laser pulses allowed the cluster ions to be formed beyond the barrier to the ion−molecule reaction, allowing the reaction to proceed to the observed products.

For most of the systems discussed in this section of the review, the primary goal of the experimental investigations performed was to gain an understanding of the influence of cluster solvation on the operative electronic state coupling. However, the dynamics of many cluster systems are likely to be related to the coupling between electronic excited states. The two final studies presented are examples of how excited-state transitions can be accompanied by other processes such as evaporation and ion-state chemistry.

5. Caging Dynamics

5.1. Overview

Alteration of excited-state dynamics of a solvated molecule by caging can occur any time the excited-state species is in close proximity to its atomic or molecular solvent. Thus, the influences of caging may influence excited-state dynamics of a species in any environment other than the isolated gas phase. In terms of clusters, the caging of molecules excited to

dissociative excited-state dynamics has been studied in depth using the pump−probe technique. On a basic level, caging in a cluster occurs when the dissociation of a molecule is inhibited by collisions between the dissociating molecular fragments and the solvent atoms or molecules of the cluster, thus removing energy from dissociating species. The dissociating species may then proceed through several channels described below.

5.2. Neutral Clusters

Some of the early ultrafast experimental studies of caging dynamics[130−132] and accompanying molecular dynamics simulations[133] were performed on the I_2Ar_n cluster system. The mixed I_2Ar_n clusters were generated by co-expansion of an I_2/Ar/He mixture through a pulse valve. The I_2 chromophore within the cluster was excited to either the dissociative Ã or bound B state by a pump pulse followed by detection by probe laser-induced fluorescence of I_2. Experiments were performed at several pump wavelengths and varying backing gas pressures to study the dependence of the dynamics on the excess energy and cluster size, respectively. As a product of these detailed studies, two principle types of direct cluster caging were determined. The first was reported to proceed as follows. Upon excitation, one iodine atom moves rapidly away from the other until it collides head-on with an Ar solvent atom; the collision removes much of the initial energy of the I atom, thus making recombination of the iodine atoms to form I_2 molecule energetically favorable. This caging mechanism resulted in the fairly rapid (fewer than 10 ps) and coherent motion of the wave packet from the electronic excited state to vibrationally excited levels on the ground-state potential-energy surface. In the alternate caging process, the atoms of the dissociating molecule undergo multiple lower energy collisions with the cluster solvent until sufficient energy has been dissipated to allow recombination on the ground-state surface. This process is expected to be slower due to the occurrence of multiple collisions and the movement of solvent molecules between the I atoms; thus, the I atoms must diffuse through the solvent before recombination can occur. Loss of coherence is expected since the energy of the initial excitation becomes randomized through the cluster.

The influence of a solvent cage on the kinetic energy of the dissociating species was investigated using a velocity-gating technique.[134,135] Clusters of iodobenzene were pumped to a dissociative state by a 275 nm laser pulse. As the dissociating I atom left the cluster, it was detected by three-photon resonant ionization with a 304.7 nm probe. In addition, the kinetic energy distribution of the ionized iodine atom was monitored to gain additional information about the energetics of the dissociation process. By gating certain regions of the kinetic energy distribution, the dynamics of I atoms released from the cluster with high and low kinetic energy could be analyzed separately.

It was found that the high kinetic energy I atoms were released from the cluster very rapidly with appearance slowing with increasing cluster size to 1.4 ps when clusters of up to eight molecules were present. This high-energy I atom is expected to have been ejected from the surface of the cluster and thus only slightly perturbed. The slowing of the dynamic rise in the I^+ signal is expected to be due to an increase in the van der Waals attraction between the I atom and cluster as the cluster size increased and therefore is uncaged.

The dynamics of the low kinetic energy I atom was reported to have a time constant of 365 ps under the condition where clusters up to eight molecules were present. The low kinetic energy and the slow rise time indicate that this I atom dissociated from within the cluster. The kinetic energy of the dissociation was reported to be removed from the I atom by collisions with the solvating molecules of the cluster. The slower caging process observed appears to be similar to the noncoherent type discussed above. The difference lies in the lack of recombination following the removal of energy from the dissociating fragments of the molecule.

Similar results were observed when I_2 was solvated in benzene clusters.[50] The cluster was excited to a state that resulted in charge transfer from the benzene to the I_2, which was followed by dissociation and loss of an I atom from the cluster. Two components were observed in the dynamics that corresponded to the ejection of uncaged (fast $\approx$ 2 ps) and caged (slow $\approx$ 20−75 ps) I atom from the cluster.

In addition to the I_2 caging systems, the dynamics of caging in methyl iodide clusters has been studied.[119,136]

Methyl iodide clusters excited to the 10s Rydberg state dissociate within 200 fs through two competing processes.[119] The processes are curve crossing to the repulsive Ã state and internal conversion to the dissociation continuum of the 6s Rydberg state. Some of the dissociating CH_3 radicals and I atoms dissipate their excitation energies through collisions with the cluster cage and are able to recombine onto the 6s Rydberg state or the lower lying ground X state. Recombination onto the 6s Rydberg state occurs on the time scale of picoseconds.

Reactions between the photoexcited chromophore and a loosely bound solvating molecule have also been observed in femtosecond time-resolved experiments of methyl iodide clusters.[136] In this experiment, a pump pulse at 277 nm was used to dissociate the methyl iodide molecule, and the reaction of the iodine photofragment with the solvating methyl iodide was monitored by ionization with a 304 nm probe pulse. The velocity-gating technique was applied to separate the fast and slow kinetic-energy components of the I^+ ions formed. Pump−probe transients of the slow I^+ ion showed an interesting delayed rise behavior. The time delay was found to be 1.4 ps, and the rise time was 1.7 ps. The delay of 1.4 ps was interpreted to be due to the formation of the transition-state complex CH_3I_2, whereas the rise time of 1.7 ps was a measure of the lifetime of the transition-state complex CH_3I_2.

5.3. Anion Clusters

To further study the detailed mechanisms of caging dynamics and the ensuing processes of solvent evapo-

ration from the cluster, mass selection of anion clusters has been implemented. The experiments on mass-selected anions can be divide into two categories: those that used dual time-of-flight mass spectrometry technique to study the evaporation processes that follow the caging event and those that use photoelectron spectroscopy to investigate electronic energy relaxation associated with the caging process.

The caging dynamics of I_2^- solvated in Ar,[137] CO_2,[137−139] and OCS[139,140] has been studied using a dual time-of-flight mass spectrometry technique. The anion cluster of interest was mass selected in the first mass spectrometer. The second mass spectrometer was employed to analyze the anion clusters that remain after the pump−probe process. The resulting ion signal was interpreted as follows. The caging process following excitation by the pump results in energy transfer to the solvent in the cluster leading to the evaporation of a few molecules from the cluster. If the probe pulse arrives before I_2^- recombination occurs, light will not be absorbed and clusters with a few atoms or molecules lost to evaporation will be detected. Once recombination has occurred, the probe pulse will be absorbed, thus leading to a second dissociation and caging event which will result in the transfer of more energy to the cluster and further evaporation. Therefore, when recombination takes place before the arrival of the probe pulse, smaller cluster fragments are detected and the appearance of the small clusters presents the dynamics of the caging process induced by the pump pulse. The observed growing in of the signal due to absorption of the probe pulse was referred to as the absorption recovery time.

I_2^- contained in Ar[141,142] and CO_2[143] clusters has been studied using a femtosecond photoelectron spectroscopy technique. In these studies, a mass-selected cluster was pumped to the dissociative $\tilde{A}$ state of I_2^-; the probe pulse then detaches an electron from the anionic cluster. The kinetic energy of this electron was measured as a function of probe delay time, thus elucidating the electronic energy relaxation resulting from the caging process.

The application of these complimentary techniques to the caging of I_2^- has provided detailed temporal and energy information about caging-induced recombination and the ensuing evaporation of solvent molecules along with the influence of solvent identity and cluster size on these dynamics. The reader is referred to a recent review[144] dedicated to cluster solvation of I_2^- and references therein for further details of this thoroughly studied system.

A recent investigation of $(O_2)_n^-$ clusters has revealed a somewhat different caging process involving dissociation and recombination of the cluster core.[145,146] Dual time-of-flight mass spectrometry coupled with the photoelectron spectroscopy technique was employed. The $(O_2)_n^-$ clusters with $n \geq 3$ have a O_4^- core where the electron is centered on a dimer of O_2 molecules. Excitation of $(O_2)_n^-$ by 800 nm light results in a charge transfer from the O_4^- core to the adjacent O_2 molecule. The charge transfer was followed within a few hundred femtoseconds by a transfer of the electron back to the now neutral O_4 core.[145] The reattachment of the electron to the O_4 core leads to dissociation and subsequent caging of the O_4^-. Dissociation was found to occur by either a direct process or by vibrational predissociation. When direct dissociation (~2 ps) was the operative process and n was larger than about 10 molecules, recombination was found to occur.[146] However, vibrational predissociation was found to occur on a longer time scale, allowing transfer of energy to the solvent molecules of the cluster. This softens the cluster and decreases its ability to aid in the recombination of the O_4^- core. Thus, as discussed for the neutral caging dynamics, the time scale and coherence of the dissociation have a strong influence on the caging and recombination process.

The study of caging dynamics has played an important role in elucidating the details of the time scale of dissociative processes and the influence of adjacent solvent species on the dissociation mechanism. A clear picture of the solvent cage surrounding an excited-state species and the mechanisms by which energy is transferred to the solvent has been gained. Additionally, much of this information is likely to be analogous to a solution-phase process since the local environment in solution is comparable to the solvent shells in clusters.

6. Metal Cluster Dynamics

6.1. Overview

Metals, in general, have countless practical uses due to a range of electrical conductivity and catalytic properties resulting in numerous applications in the areas of electronics fabrication and the activation of chemical reactions. A more detailed understanding of the quantum mechanical basis of the properties of metals should aid in tailoring these properties to new applications. Studies of the dynamics of metals clusters can elucidate details of the influence of electronic structure, bonding, and geometry on the properties of metals while introducing the factor of quantum confinement, which alters the properties of metal clusters, comprised of a small number of atoms when compared to the bulk.

6.2. Electronic Relaxation in Transition-Metal Clusters

A series of dynamics studies have been performed on small cluster anions of transition metals, namely, Pd_n^- (n = 3, 4, 7),[147,148] Pt_3^-,[149] and Ni_3^-.[150] All of these species were studied using the time-resolved photoelectron spectroscopy technique.[151] Clusters were generated by vaporization of the metal being studied in a pulsed arc cluster ion source. The anionic cluster size of interest was then mass selected using a time-of-flight mass spectrometer. The mass-selected anion clusters were pumped to an excited state by absorption of one photon from a pump laser pulse. At time intervals, the excited electron was detached from the cluster by a probe laser pulse and the kinetic energy of the photodetached electron was analyzed by a magnetic bottle electron spectrometer. The

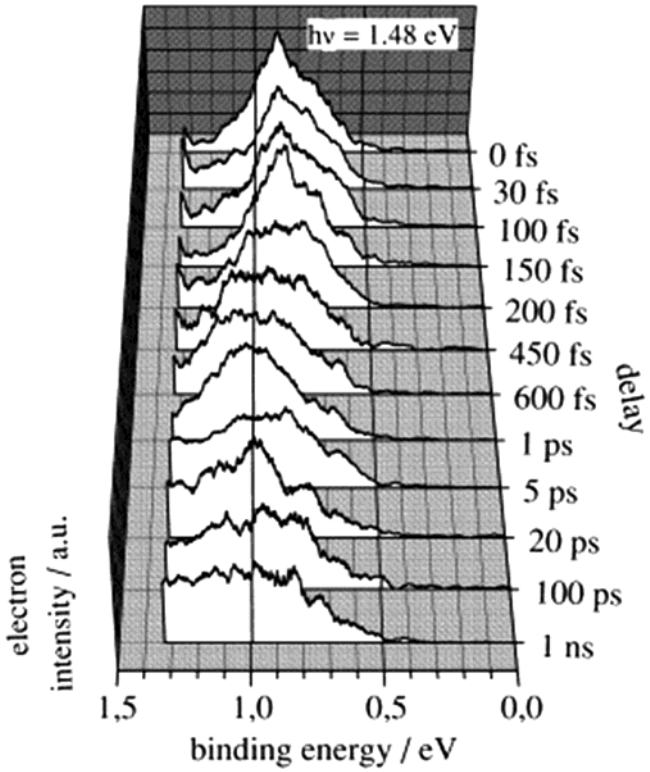

Figure 9. Time-resolved photoelectron spectroscopy data of Pd_3^- obtained using 1.48 eV pump and probe pulses. Reprinted with permission from ref 147. Copyright 2001 Elsevier.

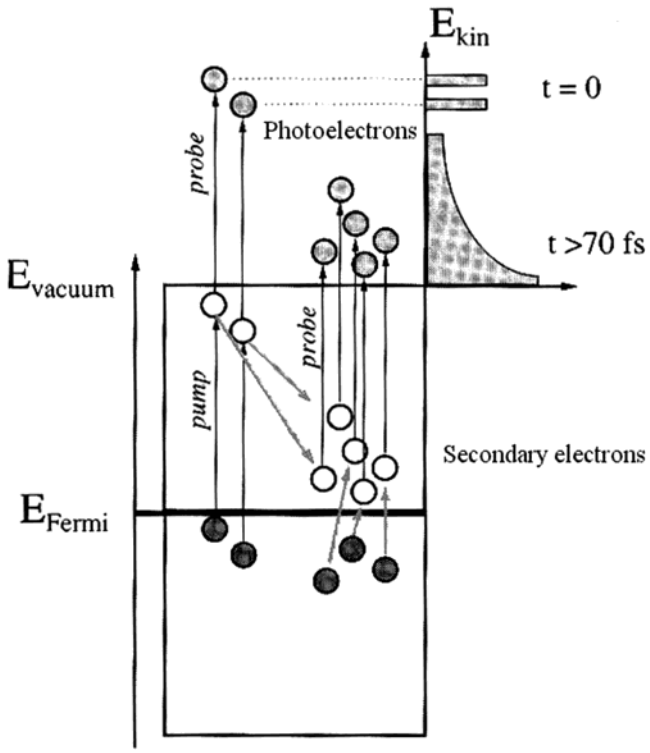

Figure 10. Schematic representation of the electron-scattering process and the influence electron relaxation has on the photoelectron spectrum. Reprinted with permission from ref 151. Copyright 2000 Springer-Verlag.

resulting time-dependent photoelectron spectrum represents the decay rate and energy of the excited-state electron.

The temporal behavior of Pd_3^- following 1.48 eV excitation and 1.48 eV electron detachment will be discussed first as its behavior is characteristic of the transition-metal clusters.[147] Photoelectron spectra of Pd_3^- taken at several pump−probe delay times are shown in Figure 9.[147] The content of Figure 9 can be more easily understood by dividing the spectra into three regions of binding energy. The signal in the 0.02−0.7 eV binding energy range results from the detachment of electrons that were in the initial high level of excitation from the pump pulse. This region undergoes a rapid decay into the higher binding energy region due to inelastic scattering of the excited-state electron with unexcited electrons in the cluster. Application of a fitting procedure to the low binding energy portion of the spectrum produces a lifetime of 90 ± 30 fs. The 0.7−1.1 eV range results from detachment of electrons that have become excited through the inelastic scattering process. This region exhibits a slower relaxation than the low binding energy electrons. The 1.1−1.48 eV region is the result of electrons that have relaxed to as low of a level as possible; this signal grows in for the first picosecond then remains constant at longer times. A graphical representation of the electron-scattering process is shown in Figure 10. In another study of palladium clusters, which resulted in qualitatively similar data, the relaxation dynamics of $n = 3$, 4, 7 clusters were investigated following excitation of 1.48, 1.54, and 1.57 eV, respectively.[148] The relaxation times of the low binding energy edge of the photoelectron spectra were found to be 42 ± 19 fs for $n = 3$, 91 ± 17 fs for $n = 4$, and 25 ± 14 fs for $n = 7$. The fast relaxation of the excited electron is the result of inelastic scattering between the excited electron and electrons below the Fermi level. Inelastic scattering in bulk metal has been found to occur in about 10 fs, significantly faster than the rates determined for the Pd_n^- clusters. The decrease in the rate of inelastic scattering in clusters is a direct consequence of the decreased density of states resulting from the small size of the clusters. The density of states argument also applies to the cluster size influence on the relaxation time. A higher state density is expected in the Pd_7^- cluster than in the smaller clusters, leading to the faster relaxation time. A comparison to the other metals studied adds conformation to the density of states argument. The studies of the Pt_3^- cluster[149] displayed a relaxation time for the low binding energy electrons of less than 70 fs, which agrees well with the Pd_n^- results since both of these metals have a large number of d orbitals, resulting in a high density of states in the cluster. Ni_3^- [150] however exhibited slower relaxation of the excited electron with a lifetime of 215 ± 50 fs due to a lower density of states in clusters of the smaller Ni atom.

The inelastic scattering process is followed by transfer of the electronic energy to the vibrational modes of the cluster. The transfer of electronic to vibrational energy was observed as a decay in the high binding energy region of the photoelectron spectra for many of the species studied. This process was found to occur with time constants of 0.7 ± 0.3 ps for $n = 4$, 1.0 ± 0.3 ps for $n = 7$ for the Pd_n^- clusters[148] but not in the Pd_3^- data shown in Figure

9. Electronic to vibrational energy transfer was also observed in Ni_3^- and found to occur with a time constant of 450 ± 150 fs.[150] An interesting study of the $Pt_2(CO)_5^-$ and Au_2CO^- clusters provides further verification of the electronic to vibrational relaxation process.[152] Upon excitation, these clusters exhibited the ultrafast relaxation of low binding energy electrons on the sub 100 fs time scale followed by the electronic to vibrational energy transfer just as observed in the pure metal clusters. However, following the transfer to vibrational energy, evaporation of a CO molecule was observed due to the vibrational energy in the clusters. The evaporation, or desorption, of the CO molecule proceeded with a time constant of 3 ± 2 ps for $Pt_2(CO)_5^-$ and 455 ± 105 fs for Au_2CO^-. The order of magnitude difference in the rate of desorption was attributed to the large difference in the number of vibrational degrees of freedom between the two clusters: $Pt_2(CO)_5^-$ has 30 and Au_2CO^- has 6.

As an interesting contrast to the very metallic behavior of the cluster systems just discussed, a study of the Au_3^- cluster revealed a molecule-like photodissociation process.[154] Upon excitation of the Au_3^- by a 3 eV photon, a dissociation process was observed that resulted in the formation of either Au_1^- and Au_2 or Au_2^- and Au_1 with the formation of Au_1^- being the dominant channel. The temporal evolution of the dissociation process was monitored by photoelectron spectroscopy of the electron detached by the probe laser. The photoelectron signal characteristic of the Au_1^- was found to grow-in with a time constant of 1500 ± 200 ps when the 3.0 eV pump was used, but the dissociation time decreased to less than 50 ps when a 3.14 eV pump was used. These observations led to the conclusion that the Au_3^- cluster has a dissociative potential-energy surface at ~3 eV which leads to the formation of Au_1^-. These dynamics are quite different from the rapid electron-scattering process observed for the transition-metal clusters.

The application of femtosecond time-resolved photoelectron spectroscopy to these metal systems allows the simultaneous determination of temporal and energetic behavior of the excited-state species. As a result, it has been possible to track the entire energy relaxation and redistribution process in these clusters, giving a complete view of the processes that follow an initial excitation in a metallic system.

6.3. Ag_3 Charge-State Experiments

As with the metal cluster systems just discussed, the Ag_3 cluster has been studied extensively using recently developed experimental techniques. One of the techniques used, referred to as NeNePo,[154] is described as it was employed to study the Ag_3 system.[154−159] Cluster anions were generated in a cold reflux discharge ion source. Then, clusters were thermalized to a desired temperature by passage through a helium-filled quadrapole ion guide and then mass selected by a quadrapole mass spectrometer. The mass-selected anionic clusters were then held in an ion trap where they were interrogated by laser pulses. Temporal measurements of the trapped anions and the derivation of the term NeNePo are the result of the following process. The pump pulse detaches the electrons from the negatively (Ne) charged cluster, leaving the cluster in the neutral (Ne) ground or excited state. At time intervals following the electron detachment, the probe pulse ionizes the neutral cluster to positively (Po) charged species that are then analyzed by a quadrapole mass spectrometer that follows the ion trap.

The silver trimer possesses an interesting property which is that the anion has a linear geometry but the neutral species takes on the geometry of an isosceles triangle and the positive ion is an equilateral triangle.[154] As a result of these structural changes with charge, the temporal behavior of the linear neutral molecule evolving into the more energetically favorable triangular neutral structure can be studied by detaching the electron from the linear anion, thus leaving the cluster in the linear neutral geometry. Using the NeNePo technique and, for example, 420 nm photodetachment and ionization laser pulses, the dynamics of the neutral ground-state relaxation from the linear to the triangular geometry has been observed. The Ag_3^+ signal was found to be at a minimum at zero delay time with the signal rising and reaching a maximum at about 800 fs. In basic terms, the initial interpretation was that the rise time in the ion signal was the time needed for the linear neutral cluster to move along the potential-energy surface toward the lower energy bent (triangular) geometry. The triangular geometry is more like the geometry of the ion-state cluster; therefore, the Franck−Condon overlap between the neutral and ion is high when the triangular geometry is reached, resulting in efficient absorption of the probe laser leading to ionization of the cluster. However, additional experimental observations indicate that other factors may be involved. When the laser wavelength was shortened, the energy was increased, the time at which the signal reaches a maximum decreased from 800 fs at 420 nm to 500 fs at 390 nm, and the decrease in time was accompanied by a decrease in signal intensity. The source of the wavelength dependence was unclear in part because the same wavelength was used for the pump and probe pulses. Thus, the wavelength dependence could have been occurring in either the photodetachment or ionization steps. Additional study of the wavelength dependence with the pump wavelength fixed at 400 nm and the probe wavelength varied from 384 to 347 nm showed the same wavelength dependence as before with the higher energy probe resulting in the ion signal reaching its maximum at earlier times.[155] This observation led to the conclusion that the shift in the time required to reach the maximum in the signal was the result of a shift in the point on the potential-energy surface where two-photon resonant ionization through the $^2E''$ excited state of Ag_3 becomes efficient. Another interesting observation was that the Ag_3 was expected to oscillate in the bound ground state, resulting in a periodic recurrence of the maximum in the ion signal as the wave packet returns to the Franck−Condon region. However, this recurrence was not observed. It was believed that as the linear cluster bends toward the triangular struc-

ture it passes through the minimum with the bond angle continuing to decrease until a strong interaction, likened to a collision, occurred between the end atoms of the cluster. This collision transfers much of the energy of the bending motion into the other vibrational modes of cluster, leading to IVR and loss of coherence in the bending motion. When the temperature dependence of Ag_3 dynamics was studied using 408 nm pump and probe pulses, it was found that the time needed to reach the maximum in the ion signal decreased with increasing temperature from 880 to 530 fs in the range from 20 to 300 K.[156] A classical mathematical model was presented as an approximation of the influence of cluster temperature on the wave packet. The potential-energy surface and molecular dynamics studies[157,158] are referenced to for a detailed analysis of the influence of temperature.

When a coherent excited-state wave packet was produced, the result of the pump−probe experiment may display oscillations in the signal intensity, resulting in the movement of the wave packet in and out of the Franck−Condon region. Although this was not observed in the case of the Ag_3 cluster due to the rapid loss of coherence, these oscillations have been observed in many systems such as the Ag_4. The Ag_4 was studied using the NeNePo technique under experimental conditions similar to those described above.[159] The neutral excited-state cluster was generated by photodetachment of an electron from the anion by one photon of 385 nm light. Ionization by the probe laser revealed the oscillatory nature of the excited-state wave packet. A Fourier transform of the time domain data produced a frequency domain spectrum containing eight peaks that were assigned as vibrational levels of a single vibrational mode and two other peaks that were not assigned. Analysis of the vibrational frequencies led to the proposal that they result from excitation of either the $^3B_{1g}$ or $^1B_{1g}$ excited state of the Ag_4 cluster.

The second experimental technique used to study Ag_3 involves many of the steps employed in NeNePo, but the details of the apparatus are quite different.[160] Cluster anions were generated by a pulsed discharge argon ion-sputtering source which was followed by a liquid nitrogen cooled nozzle. A time-of-flight mass spectrometer equipped with a mass gate was used to select the cluster anion of interest. The electron was detached from the anion to generate neutral clusters, which were then probed as a function of time with a second laser pulse. Following the laser interaction region, the cluster beam contained positively, neutral, and negatively charged species. A positively charged reflectron was positioned in the cluster beam that reflects the cations to a detector, allowing neutral species to pass through to a second detector and deflecting the anions off axis so that they did not collide with the neutral detector. This clever use of a reflectron allowed complete analysis of the products of the pump−probe experiment with a relatively straightforward experimental setup. Photodetachment−photoionization experiments using the same wavelength for the pump and probe pulses in the range of 404−415 nm confirmed the temporal results of the first NeNePo experiment and verified

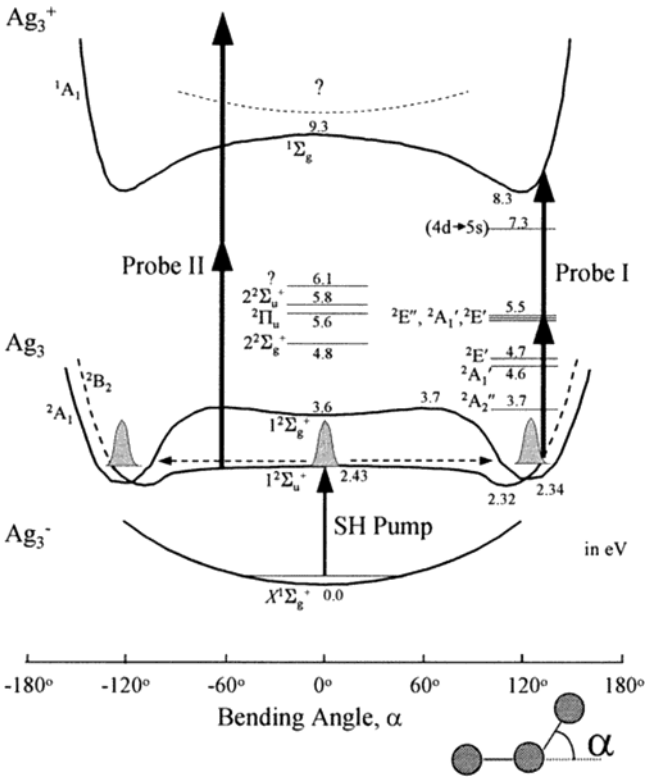

Figure 11. Schematic potential-energy surface that represents the change in equilibrium bond and angle of the silver trimer with charge and the influence of probe wavelength on the experimental results. Reprinted with permission from ref 160. Copyright 1997 American Chemical Society.

that the two- photon ionization proceeds through a resonant intermediate state. However, a study that used a pump in the 400 nm range and probe wavelengths of 269, 273, and 277 nm resulted in dynamics strikingly different from those observed with the ∼400 nm probe. These experiments resulted in a maximum in the signal at zero delay rather than a minimum, as observed in the 400 nm probe experiments. The highest signal intensity of the three wavelengths was obtained with the 277 nm probe. It was suggested that these observations indicate that an intermediate state in the two-photon ionization process has a linear geometry with an energy corresponding to 277 nm. The presence of a linear excited state would explain the strong absorption of probe photons by the linear cluster produced at the zero by the photodetachment pump pulse. The difference between the two probing schemes is indicated on a schematic potential-energy surface depicted in Figure 11. There was another interesting observation: at all three wavelengths the minima in the signal intensity were found to be at 1.5 ps. Since the time dependence of the ion signal was strongly dependent on the probe wavelength with the exception of the minimum at 1.5 ps, it was suggested that the minima was the result of movement of the ground-state wave packet rather than resonance with the intermediate state on the two-photon ionization.

The studies of transition-metal clusters and the silver trimer experiments are examples of some of the most recent work directed toward the study of metal clusters. However, it should be pointed out that

a number of other metal cluster systems have been performed that were not discussed here because they have been covered in previous review articles that focused on the study of metal cluster dynamics.[161,162] Some of the omitted experiments include studies of Na_n,[163−178] K_n,[178−183] NaK,[184] and other studies of Ag_n[162] clusters.

7. Electronic Excitation, Relaxation, and Ionization of Met-Cars

7.1. Overview

Several years ago during the course of undertaking detailed studies of dehydrogenation reactions of hydrocarbons induced by titanium ions, atoms, and clusters, the formation of an unusually abundant and stable cationic species having a molecular weight of 528 amu was discovered, which thereafter was established to contain 8 titanium atoms and 12 carbons.[185−188] Subsequent work revealed the existence of the neutral molecular cluster, its anion analogue, the stability of other transition metal−carbon complexes of identical stoichiometry, and thereafter a general class of caged molecular clusters comprised of early transition metals bound to carbon atoms in the same stoichiometric ratio,[185−231] M_8C_{12} (where M denotes an early transition metal). These have been termed metallocarbohedrens or Met-Cars for short.

Early findings based on titration experiments showed a smooth uptake of eight bonded ligands, implying that each of the titanium atoms was identically coordinated, i.e., bonded to three carbon atoms through Ti−C bonds, with each of the carbons also bound to its adjacent carbon through a double bond.[207−211,232−235] This led to the suggestion that this species (as well as its corresponding neutral molecule discovered later) might have a pentagonal dodecahedron structure. Since then a variety of structures in addition to the pentagonal dodecahedron have been considered theoretically,[212−218,236] and more recent experiments and theory tend to support a T_d, D_{2d}, or C_{3v} structure[231,237] rather than the originally proposed one of T_h symmetry.[185]

7.2. Delayed Ionization

One of the interesting features of Met-Cars is the large degree of delayed ionization, which they undergo when subjected to pulsed lasers of nanosecond time dimension. The phenomenon of delayed ionization in clusters has been reported for several systems including the Met-Cars,[223−225,244] pure transition metals,[238−240] metal oxides,[241−243] metal carbides,[243] and the fullerenes.[245−248] Recent developments show that the delayed ionization of fullerenes diminishes dramatically as the laser pulse width is reduced to femotoseconds.[247] Currently there is considerable interest in the origin of the various operative phenomena, prompting extensive theoretical and experimental investigations for various systems. In order for a cluster to display delayed ionization in a manner analogous to bulk-phase thermionic emission,[249] the ionization potential of the cluster must be less than its dissociation energy and all of phase space must be accessed by the system. The first requirement ensures that ionization, as an energy dissipation mechanism, will be more favorable than dissociation. Theoretical calculations and experimental results show that Met-Car clusters meet this requirement. The second requirement enables the system to temporarily store energy in excess of the cluster's ionization potential through statistically sampling a large number of accessible vibrational and electronic states.

Studies conducted in the Castleman laboratory employing nanosecond lasers revealed that some degree of ionization occurred on a time scale orders of magnitude longer than that which is characteristic of normal photoionization that obeys the photoelectric effect. In order for the delayed ionization to be observed for Met-Cars, the clusters must have some way to accommodate the energy necessary for the ionization to occur while at the same time not undergo dissociation into smaller cluster fragments. Metallocarbohedrenes are thus ideal systems to exhibit this behavior, because when comparing the experimentally measured ionization potential (IP) and the theoretically predicted value for the dissociation energy (E_{diss}), a favorable relationship ($IP/E_{diss} < 1$) exists for this family of cluster molecules. This favorable relationship and the large density of electronic states for these transition-metal−carbon species may allow for the clusters to "store" the energy gained during the excitation and delay ionize on a long time scale characteristic of the experiment.

In order for the delayed ionization to be well described by the thermionic emission model, adequate time must be available for the energy associated with the electronic excitation to be distributed throughout all accessible states, namely, that there is sufficient time for all of phase space to be sampled. In the case of excitation via femtosecond laser pulses, the time between successive absorptions may be insufficient for this requirement to be attained.

7.3. Ultrafast Dynamics

To shed further light on the phenomena involved, femtosecond pump−probe experiments have been performed on vanadium Met-Cars.[226,227] A comparison between the lifetimes of V_mC_n clusters and the vanadium Met-Car were performed. In addition, the influence of pump wavelength on the excited-state lifetime has been explored.

The femtosecond dynamics of vanadium−carbon clusters generated from a laser vaporization source were investigated employing 400 nm pump and 620 nm probe laser pulses and detection by mass spectrometry.[226] Fitted transients for a series of vanadium−carbon clusters, including V_8C_{12}, are presented in Figure 12. The Met-Car response with a fitted width of 225 fs (fwhm) is noticeably longer than the autocorrelation width of the laser pulses with a cross correlation measured to be ≤86 fs. This measurable difference indicates that a state (or band of states) with an appreciable lifetime was being accessed. Since these clusters are strongly bound,[202] the pump−probe response is likely too short to be attributable to a fragmentation process, either in the Met-Car

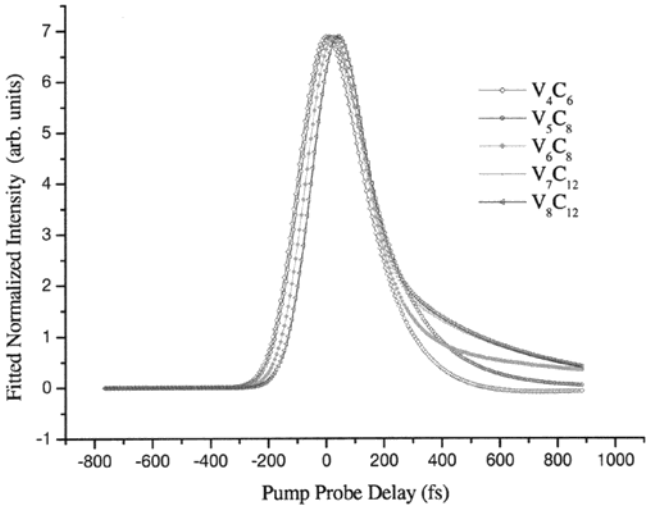

Figure 12. Fitted pump−probe transients of the vanadium−carbon clusters: V_4C_6, V_5C_8, V_6C_8, V_7C_{12}, and V_8C_{12}. Pump: 400 nm, 50 fs, 24 mJ. Probe: 620 nm, 50 fs, 20 mJ. Reprinted with permission from ref 226. Copyright 2001 American Chemical Society.

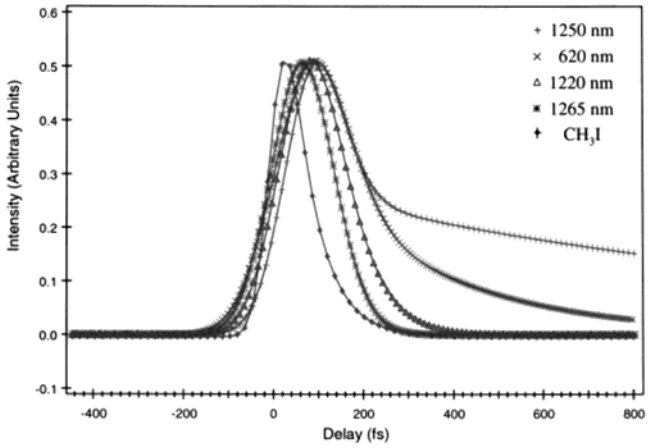

Figure 13. Normalized pump−probe fit comparison for V_8C_{12} as the implemented wavelengths are tuned closer in resonance with an excited electronic state or band of coupled states. The fitted response for CH_3I is reproduced for comparison. Reprinted with permission from ref 227. Copyright 2002 American Institute of Physics.

cluster or in larger clusters that might be thought of as possible contributors to the formation of a Met-Car. The pump−probe response was thus attributed to the temporal dependence of the electronic relaxation behavior of this system.

Another significant observation is the fact that the pump−probe transients for all of the observed vanadium−carbon clusters with more than four metal atoms show a similar pump−probe response. They display exponential decays on the order of a few hundred femtoseconds. This observation suggests that there is a common chromophore[226] present in clusters, likely to be the V_4C_x series. It is also important to note that the excited-state lifetimes become shorter as the cluster size increases. This result suggests that the larger nanoscale complexes have increasingly more free-electron character, and therefore, the rate of energy relaxation is higher in the larger clusters. The long-time tail in the Met-Car spectrum suggests relaxation into a state or band of states.

Similar relaxation behavior was observed at other wavelengths as well. For example, a typical pump−probe transient of the vanadium Met-Car pumped at moderate laser fluence by a range of wavelengths and ionized by an 800 nm probe is shown in Figure 13.[227] These findings begin to reveal the large density of excited electronic states involved and the concomitant effect on the relaxation dynamics. Observations indicate that small changes in the pump wavelength dramatically affect the behavior of the system. Through the interpretation of previous findings and those presented below, excitation was believed to occur via a sequential absorption of two pump photons of the IR pump (or one photon for the 620 nm pump experiment) followed by the absorption of three 800 nm photons to surpass the ionization potential. Figure 13 contains a trace of CH_3I as an indication of the cross-correlation width of the laser pulses used. It can be seen in the temporal behavior of the Met-Car that the maxima in the signals are shifted relative to each other with the shift having noticeable wavelength dependence and that Met-Car signals have a broader width than that of CH_3I. In addition, a tail is observed from 200 fs to the end of the time window studied for some pump wavelengths. In terms of both the signal maximum and the longer time tail, the 1250 nm pump results in the longest lifetime of the Met-Car excited state. Since the IR pumping is expected to involve a two-photon absorption, the 620 nm pump experiment results in an excitation of slightly higher energy than that of the 1250 nm pump. This small increase in energy results in a decrease in the excited-state lifetime as can be seen by comparing the decays of the tail in the pump−probe transients. Increasing the pump energy by shortening the pump wavelength to 1220 nm confirms the trend with a further decrease in the excited-state lifetime. When the pump wavelength was increased from 1250 to 1265 nm, decreasing the pump energy, the shortest excited-state lifetime was observed as evidenced by the maximum in the signal being closest to that of the CH_3I and a nearly absent tail at longer times. These data indicate the presence of an excited state or band of states in the region of 2 eV that leads to the increased lifetimes when the excitation energy is in this region.

The dynamics studies provide clear evidence for electronic energy coupling to lattice modes being operative, with findings that at long delay times the latter could contribute to the thermionic emission that has been observed. Importantly, these new findings show that the delayed ionization process, typically seen only under excitation via nanosecond pulses, might be revealed in experiments conducted with laser fluences that enable relaxation into electronic bands during a femtosecond excitation process. This work is providing a new understanding of the process generally termed “thermionic” ionization/emission, in terms of the microscopic quantum effects of the influence of the dynamics of relaxation into electronic bands that govern the temporal characteristics of the phenomena.

In addition to revealing the time-resolved behavior of V_8C_{12}, studies focusing on the relative dynamics

of V_6C_8 were also conducted. Interestingly, upon inspection of the findings in Figure 12, the fitted transient widths have become slightly narrower with the increase in cluster size. This observed decrease in electronic relaxation time (fwhm), relative to the smaller clusters, is indicative of the increased free electron character that was previously observed in the Met-Car species under 620/400 nm in that electron−electron and electron−phonon relaxation is more efficient, thus yielding shorter dynamics under conditions where specific states are not being accessed. With the vast number of electrons dictating the behavior observed in these clusters, relaxation from presumably closely spaced excited states would likely occur on a short time scale (subpicosecond) given the vast number of electrons involved and the subsequent interaction and energy redistribution processes. Also given the low ionization potential of the Met-Car (V, 5.5 eV; Ti, 4.40 eV; Zr, 3.95 eV) compared with the ionization potential of the constituent metal (V, 6.74 eV; Ti, 6.82 eV; Zr, 6.84 eV) and carbon (11.26 eV), these species contain relatively increased delocalized electron character, in comparison to species of smaller size, and the subsequent relaxation processes likely include efficient electron−phonon coupling and electron−electron scattering.[238,250]

8. Phenomenon of Coulomb Explosion

8.1. Overview

Coulomb explosion (CE) is a class of reactions that has been observed when clusters become multiply charged.[251−258] Ionization involving multiple electron loss is not new, having been first observed in various systems ionized via electron impact techniques. In most of these experiments, metastable clusters containing one, two, or three charge centers were produced. The metastability arose only in systems of sufficient size that the charge centers could separate by a large enough distance to reduce the Coulomb repulsion to a magnitude that did not exceed the cohesive binding energy of the cluster. Early examples include clusters composed of CO_2,[251] various metal atoms such as those of the alkali metals,[252] hydrogen-bonded systems such as water and ammonia clusters,[253,254] and rare-gas clusters.[255,256] Below a critical cluster size, however, fission leads to the loss of the multiple charges from a cluster and hence to the production of several singly charged species. Metastable evaporation of the solvating molecules can take the stable cluster to degrees of aggregation below critical size and subsequently lead to fission. Findings concerning the phenomenon of Coulomb explosion come from a plethora of investigations of the interaction involving intense laser fields with atoms,[259−265] molecules,[266−271] and clusters.[272−283]

High-flux femtosecond laser pulses provide short bursts of light, leading to the delivery of many photons to the cluster and almost instantaneously the loss of many electrons. These initially ionized free electrons can further ionize the inner-shell electrons of the atomic constituents of the cluster via intracluster inelastic electron−atom collisions. During the photon absorption and subsequent ionization processes, there is little time for nuclear motion. The highly charged atomic ions of the cluster are formed in very close proximity, and hence, the system thereafter rapidly explodes due to the Coulomb repulsion between the atomic ions of like charges, releasing atomic ions with high kinetic energies.[272−274] Early studies of CE induced by femtosecond laser pulses, showing the role of clustering, were reported by Castleman and co-workers[272−274] for high charge state species generated in ammonia clusters and in xenon clusters where high charge states in xenon were reported by Rhodes and co-workers[280−283] at about the same time. As mentioned below, the exact mechanisms leading to the phenomenon are a subject of intense current interest among theoreticians as well as experimentalists.

8.2. Models of the CE Process

Several theoretical approaches have been introduced to model the CE process in molecules and clusters. Among them are the ionization ignition model (IIM), the coherent electron motion model (CEMM), and the charge resonance-enhanced ionization (CREI). In all these models, barrier suppression plays an important role in the first stage of cluster ionization. For a laser beam with an intensity of $\sim 10^{15}$ W/cm^2, the field strength is on the order of 10 V/Å, which is strong enough to field ionize at least one of the valence electrons of all the nuclei in the cluster.

In the IIM picture,[280,281] at the very beginning of the ionization events, the nuclei in the cluster are considered frozen while the ionized electrons are quickly removed from the cluster by the laser field. Even in small clusters, the unshielded ion cores in the cluster produce a very large (>102 V/Å) and inhomogeneous electric field. This large field lowers the ionization barrier and facilitates subsequent ionization processes, which in turn further lowers the ionization barrier. According to the IIM model, the field created by the initial ionization event "ignites" the cluster, which causes the further ionization processes. The model predicts that multiple ionization is strongly dependent on the cluster density but is not very sensitive to either the atomic weights of cluster constituents or the pulse duration of the laser beam, as long as the same intensity can be obtained.

In the CEMM model,[282−285] interaction between the laser field and clusters can enter a regime of strong electromagnetic coupling which arises from the coherent motion of the field ionized electrons (Z) induced by the external laser field. These coherently coupled electrons behave like quasi-particles, each with a charge Ze and a mass Zm_e. Subsequent ionization can be envisioned as the electron impact ionization by these coherently energized electrons. According to the CEMM model, the ionization rate of the cluster increases with cluster size but decreases with internuclear distances. This is in contrast to the CREI model,[280,281,286−292] which predicts that the rate of ionization is a highly irregular function of the internuclear distance.

In the CREI model for diatomic molecules,[286−292] an inner potential barrier existing between the two

nuclei rises with the internuclear distances. The electron motion between the two nuclei slows down due to the barrier. At a certain critical distance, when the characteristic frequency of the electron motion becomes in resonance with the laser, the electron energy is enhanced leading to an enhanced ionization rate. A dynamic CREI model was later proposed by Jortner and co-workers,[294−296] in which the electron energy was shown to increase roughly at the same rate as the level of the barrier height. The dynamic model predicts higher ionization efficiency than the static CREI model.

8.3. Experimental Studies of CE

Several different types of experiments have provided definitive evidence for the role of clusters in effecting the facile formation of highly charged species at modest laser fluences. The first conclusive evidence was obtained from experiments employing a covariance analysis approach.[261,297] Probing various cluster distributions in a pulsed molecular beam and correlating the findings of high charge state formation with cluster size through covariance methods has served to further elucidate the mechanisms responsible for the generation of multiply ionized constituents.

Other direct evidence for the role of clusters has been acquired in a series of experiments conducted in a manner which focused on the composition of the molecular beam which produced the most intense highly charged species at a given laser fluence.[278,279] One experiment involved fixing the focal position and changing the delay of the pulse nozzle relative to the laser pulse. This experiment enables scanning of the entire neutral cluster and unclustered molecule packet. Several different factors were examined: charge-state distribution, kinetic-energy release, and integrated signal intensity as a function of the delay between the laser and pulsed valve. All three exhibited the same trend, namely, showing that the high-charged species were only present and with high kinetic-energy release when clusters dominated the beam. Essentially no highly charged species were observed when monomer alone was present, even at very high concentrations and laser intensities.

In various experiments[274,278,279,307] on small clusters, multicharged atomic ions resulting from the CE process were observed only when a certain minimum cluster size was reached, and the charge distribution does not vary significantly with further variation in the cluster distribution. For example, with a laser power of $\sim 10^{15}$ W/cm^2, pure xenon, ammonia, and acetone clusters were found to readily undergo the CE process whereas krypton and argon clusters did not, unless a trace amount of HI or another low IP species was doped in the clusters. The fact that under the laser power employed in these experiments neat Kr (IP = 14.00 eV) and Ar (IP = 15.76 eV) clusters did not exhibit multiple ionization whereas neat Xe (IP = 12.13 eV), HI (IP = 10.39 eV), NH_3 (IP = 10.18 eV), and $(CH_3)_2CO$ (IP = 9.71 eV) clusters did suggests that multiple ionization of clusters is less sensitive to atomic number of the cluster constituents and depends more upon the threshold for single ionization. These results are in general agreement with the IIM model predictions.

Particularly interesting findings first came from studies of molecular clusters,[272−274] including $(NH_3)_n$, $(HI)_n$, X_n (X = Ar, Kr, Xe), and $(CH_3COCH_3)_n$, etc. In the case of $(HI)_n$ clusters irradiated with a femtosecond laser at 624 nm and a power of $\sim 1 \times 10^{15}$ W/cm^2, prominent peaks corresponding to multicharged I^{n+} ions were observed, with $n = 17$ being clearly discernible[273] and indicating the loss of all valence electrons. A broad peak was found for the multicharged fragments having an early arrival time, followed by a sharp peak arising from space focusing for those species corresponding to a later time of arrival. The kinetic energy measured by the peak splitting along with those determined employing a retarding field energy analyzer has generally been found to be in good agreement. The high values of several hundred to several thousand electronvolts which were measured for the ionization of HI clusters cannot arise from the CE of HI monomer because they would necessitate unallowably small internuclear distances between H^+ and I^{n+}. This finding indicated that the large kinetic energies observed in the study result from the CE of HI clusters, a conclusion born out by the covariance studies and other more direct experiments.

Another aspect of the CE process has been learned from the study of acetone clusters[274] where highly charged carbon and oxygen atoms were found to be produced. A unique feature of the work performed on this system was the utilization of pump−probe techniques in the ionization process as a test of theoretical predictions of the possible mechanisms involved. In this case, the pump laser at 624 nm has a power density of $\sim 3 \times 10^{14}$ W/cm^2 and the probe laser also at 624 nm was slightly (~10%) weaker. The pump−probe transients of the oxygen fragments (O^{n+}, $1 \le n \le 5$) are shown in Figure 14. There are several significant features that should be noted. A large dip was observed in the O^+ transient at zero delay, and a peak begins to grow in for each subsequently higher charged species. For the higher charged species (O^{n+}, $2 \le n \le 5$), the ion signal drops to a local minimum and then returns to a local maximum at some pump−probe delay. At longer delay times, the O^{n+}, $3 \le n \le 5$, show clear signs of an oscillatory pattern. The unequal intensities of the maxima at positive and negative delay times can be attributed to the unequal pump and probe intensities, but significantly, the maxima in O^+ and O^{5+} occur at positive delay times, whereas the maxima in O^{2+}, O^{3+}, and O^{4+} occur at negative delay times. C^{n+} ($1 \le n \le 4$) observed in the experiment was found to behave in a similar fashion. These findings point to the acquisition of some quantum control in the area of high-intensity laser irradiation of clusters, a prospect which has now been realized in molecules by Levis and Rabitz.[303,304] The observed oscillating pattern could not arise from the phasing of the pump and probe optical fields since the period of the laser was about 2 fs. Bear in mind that the power of either the pump or probe beam was sufficient to multiply ionize the acetone clusters. Following the pump

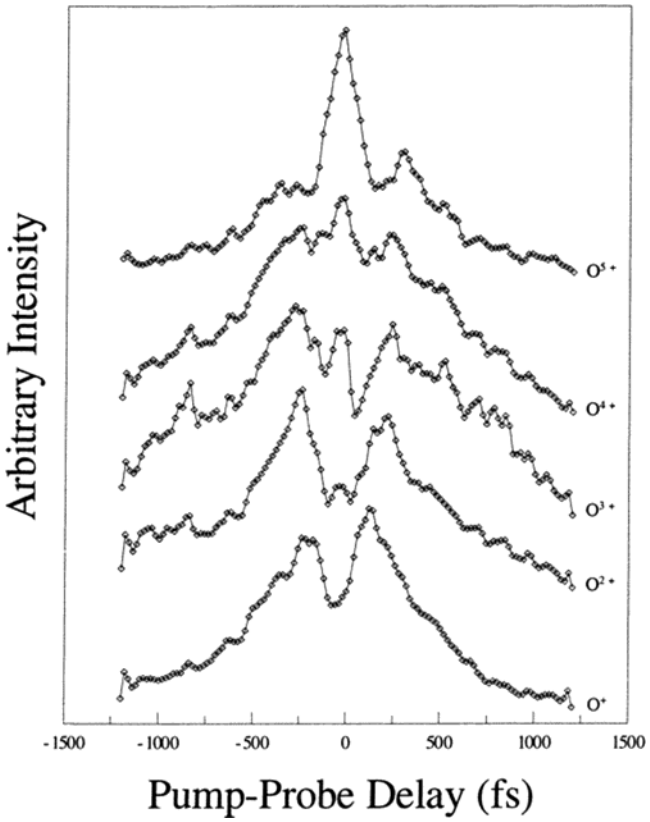

Figure 14. Pump−probe transients of oxygen atoms with multiple charges produced by the Coulomb explosion of acetone and acetone clusters. Reprinted with permission from ref 274. Copyright 1996 American Physical Society.

pulse, the acetone cluster undergoes multiple electron loss and the probe beam arrives at the cluster at some later time. Depending on the time delay of the probe beam the interatomic spacing increases, as predicted by Bandrauk,[298−300,289−293] Corkum,[286,287,301] Jortner,[294−296] and co-workers. As the interatomic spacing varies, the wave function and electron localization was changed. According to the CREI model, this would result in different ionization rates for the various charge states, thus yielding the beating pattern seen in the experiments.

Studies of van der Waals and hydrogen-bonded clusters irradiated by femtosecond laser pulses indicate that the high charge states obtained are well described by both the IIM and CREI models. The lack of dependence on atomic weight and the strong dependence on ionization potential and internuclear distances support this conclusion. Present results cannot totally eliminate the possibility of coherent electron motion, but under experimental conditions of intermediate laser power and small cluster size, it does not appear to be a major contribution to the multiple ionization and subsequent CE process.

8.4. Chemical Applications of Coulomb Explosion

The ability to selectively dissociate molecules via CE has been developed into a technique termed CE imaging, which takes advantage of this phenomenon to gain information on the time evolution of the reaction intermediates.[92,93] In the CE imaging technique, the first femtosecond laser pulse was employed to launch the system to an excited state of interest. The second intense femtosecond laser pulse was used to initiate the CE process in the reaction intermediates, and the Coulomb-exploded fragments were detected at defined delay times. Calculations[302] have placed the approximate separation times of the multiple-charged species in the neighborhood of 25 fs, so that little change occurs after the initial CE event. Therefore, information regarding the reaction intermediates can be extrapolated from the time-resolved detection of fragments. This technique was successfully applied to the study of the tautomerization reaction in the 7-azaindole dimer,[92,93] as discussed in the section on double proton transfer and depicted in Figure 15.[92,93]

A new technique (MEKER; minimum excess kinetic energy required for an ion to be detected) has been developed that employs a time-of-flight mass spectrometer (TOF-MS) for the analysis of high-energy multicharged cations produced by CE.[305] MEKER can be employed in the study of the multicharging process in clusters affected by relatively modest laser fluences. Additionally, MEKER can be implemented to assist in furthering the development of the use of CE for arresting intermediates in fast reactions. MEKER employs energy gating through a manipulation of electric potentials in the Wiley−McLaren lens assembly and the use of a reflecting electric field. As part of a test case, water clusters of sizes up to about 20 molecules were irradiated with femtosecond laser pulses to generate protons and multicharged oxygen atoms.

The magnitude of kinetic-energy release in CE can exceed the capabilities of the electronics in a TOF-MS when operating under typical voltage settings. The TOF gating method removed the low or zero kinetic-energy ions and slowed high-energy ions in a controlled manner for facile detection. Kinetic-energy release values for O^{4+} of greater than 13 kV were reported arising from water clusters.[305] Maximum proton kinetic energy release was determined to be greater than 3 kV. Furthermore, comparisons of the TOF gating study were made with previous methods for determining kinetic energy release, the cutoff, and the peak splitting methods. The average kinetic energies determined from these methods are actually the average kinetic energy of the detected species. The high-energy species are lost either by collision with the first TOF acceleration grid (backward ejected ions) or by passing through the reflectron (forward ejected ions).

Studies of methanol clusters were made for comparison with the water cluster results.[305] The resulting high-charged species (C^{2+}, C^{3+}, O^{4+}) acquired large amounts of kinetic energy resulting from Coulomb repulsion of multicharged atomic ions that reside in close proximity to one another. Protons, which were of two kinds, namely, methyl and hydroxyl, also acquire large amounts of kinetic energy. When compared with protons generated from the CE of water clusters ($(H_2O)_n$, $n \leq 20$), protons from methanol clusters ($(CH_3OH)_n$, $n \leq 10$) acquire less overall average kinetic energy, which is in agreement with earlier findings that suggest greater clustering

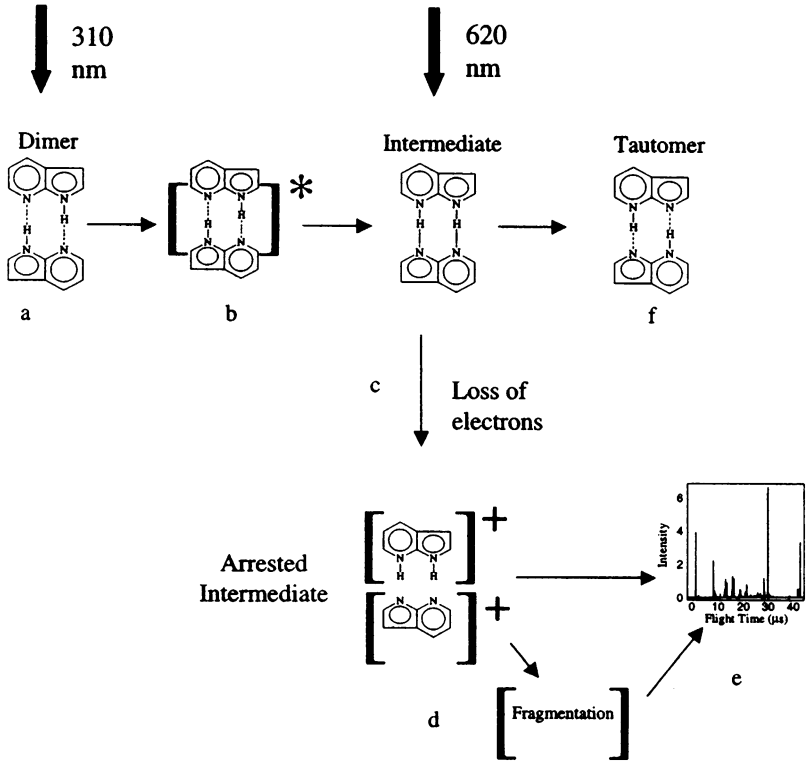

Figure 15. Schematics of Coulomb explosion imaging technique. (a) The 7-azaindole dimer was excited by a 310 nm femtosecond pulse. (b) The excited half of the 7-azaindole initiates the tautomerization process. (c) A second 620 nm femtosecond pulse Coulomb explode the intermediate. (d) The 119 amu fragment was ionized in the CE process, while the 117 amu half was unstable and fragments into several low-mass charged species. (e) Cations were detected in a time-of-flight mass spectrometer. (f) Full tautomerization proceeds if the 7-azaindole dimer was not interrupted by Coulomb exploding 620 nm pulse. Reprinted with permission from ref 93. Copyright 2000 Elsevier.

yields higher energy. Interestingly, despite the lower average kinetic-energy released, the methanol protons peak at a higher value of energy than those generated in the water cluster system, an effect attributed to the presence of both methyl and hydroxyl groups.

Irradiation of clusters with intense laser field offers other potential applications as well, for example, the generation of ultrafast X-ray pulses and tabletop fusion experiments and the resulting production of neutron beam. Rhodes and co-workers measured very efficient X-ray emission in rare-gas clusters excited with intense laser field. They predicted that the emission time for kilovolt hard X-rays could be subpicosecond and control of the pulse width and wavelength of the X-ray may be possible through molecular design.[306] With the inclusion of this coherent electron motion, Rhodes and co-workers were able to explain their experimentally observed L- and M-shell X-ray emission from Xe and Kr clusters ($n \approx 100$) exposed to laser powers in the range of $10^{16}-10^{19}$ W/cm^2 using the CEMM model. These findings may lead to the ultimate development of ultrafast X-ray lasers, which could provide real-time imaging with molecular resolution. Ditmire and co-workers[275-277] observed the $D + D \rightarrow He^3 + n$ fusion reaction when high-energy deuterium ions (>keV) were created by the interaction of an intense laser field ($\sim 2 \times 10^{16}$ W/cm^2) with deuterium clusters. An efficiency of about 105 fusion neutrons per joule of incident laser energy was obtained, which approaches the efficiency in large-scale laser-driven fusion experiments. This result shows the possibility of developing tabletop fusion experiments using small-scale laser systems, which could lead to the development of tabletop neutron source, which could find a wide range of applications in various fields.

9. Outlook

As is evident by the extent of research presented in this review, the field of gas-phase cluster dynamics is a diverse one that reaches into many aspects of fundamental and application-driven science. Information gleaned from the study of metal and semiconductor clusters have promise in applications in nanotechnology. As already been stated, proton/hydrogen transfer processes and hydrogen bonding are of central importance in biological systems, and knowledge of fundamental mechanisms of acid dissolution and photochemistry contribute to a more detailed understanding of atmospheric chemistry. Of equal importance, studies involving the investigation of the properties of electronic excited states aid in the ever-increasing understanding of quantum systems, particularly when solvation is expected to play an important role. The systems discussed in this review and the myriad of other potentially interesting systems promise to keep vital the field of cluster science for years to come.

10. Acknowledgments

Financial support by the U.S. Air Force Office of Scientific Research, Grant No. F49620-01-1-0122, the

Atmospheric Sciences and Experimental Physical Chemistry Divisions of the U.S. National Science Foundation, Grant No. NSF-0089233, and the Department of Energy, Grant No. DE-FG02-97ER14258, is gratefully acknowledged.

11. References

(1) Castleman, A. W., Jr.; Keesee, R. G. *Chem. Rev.* **1986**, *86*, 589.
(2) Castleman, A. W., Jr.; Keesee, R. G. *Science* **1988**, *241*, 36.
(3) *Clusters of Atoms and Molecules*; Haberland, H., Ed.; Springer-Verlag: Berlin, Heidelberg, 1994.
(4) Miller, R. E. *Acc. Chem. Res.* **1990**, *23*, 10.
(5) *Reaction Dynamics in Clusters and Condensed Phases*; Jortner, J., Levine, R. D., Pullman, B., Eds.; Kluwer Academic: Dordrecht, Holland, 1994.
(6) Bernstein, E. R. *Annu. Rev. Phys. Chem.* **1995**, *46*, 197.
(7) Castleman, A. W., Jr.; Bowen, K. H., Jr. *J. Phys. Chem.* **1996**, *100*, 12911.
(8) Castleman, A. W., Jr. In *Advances in Gas-Phase Ion Chemistry*; Babcock, L. M., Adams, N. G, Eds.; JAI Press: Stamford, CT, 1998; Vol. 3, p 185.
(9) *Large Finite Systems*; Jortner, J., Pullman, A., Pullman, B., Eds.; Reidel Publishing Co.: Boston, 1987; Vol. 20.
(10) *Physics and Chemistry of Small Clusters*; Jena, P., Rao, B. K., Khanna, S. N., Eds.; *NATO ASI Series B: Physics*; Plenum: New York, 1987; Vol. 158.
(11) *Elemental and Molecular Clusters*; Benedek, G., Martin, T. P., Pacchioni, G., Eds.; Springer-Verlag: New York, 1988.
(12) Schuster, P.; Wolschann, P.; Tortschanoff, K. In *Chemical Relaxation in Molecular Biology*; Pecht, I., Rigler, R., Eds.; Springer-Verlag: New York, 1977; p 107.
(13) Castleman, A. W., Jr.; Mark, T. D. *Adv. At. Mol. Phys.* **1984**, *20*, 65.
(14) Castleman, A. W., Jr.; Mark, T. D. In *Gaseous Ion Chemistry/ Mass Spectrometry*; John Wiley and Sons: New York, 1986; Chapter 12, p 259.
(15) *Elemental and Molecular Clusters in Materials Science*; Benedik, G., Martin, T. P., Pacchioni, G., Eds.; Springer-Verlag: Berlin, 1987; Vol. 6.
(16) *The Structure of Small Molecules and Ions*; Naaman, R., Vager, Z., Eds.; Plenum: New York, 1988.
(17) *Ion and Cluster Spectroscopy and Structure*; Maier, J., Ed.; Elsevier Science: New York, 1989.
(18) *Atomic and Molecular Clusters*; Bernstein, E. R., Ed.; Elsevier Science: New York, 1990.
(19) Castleman, A. W., Jr. *Int. J. Quantum Chem.* **1991**, *25*, 527.
(20) *Clustering Phenomena in Atoms and Nuclei*; Brenner, M., Lonnroth, T., Malik, F. B., Eds.; Springer-Verlag: New York, 1992.
(21) Castleman, A. W., Jr. *Advances in Mass Spectrometry*; Elsevier Science; New York, 1992; Vol. 12, p 167.
(22) Castleman, A. W., Jr. *Int. J. Mass Spectrom. Ion Processes* **1992**, *118*, 167.
(23) Stanley, R. J.; Castleman, A. W., Jr. In *Molecular Dynamics and Spectroscopy by Stimulated Emission Pumping*; Dai, H. L., Field, R. W., Eds.; World Scientific: River Edge, NJ, 1995; p 689.
(24) Castleman, A. W., Jr.; Wei, S. *Annu. Rev. Phys. Chem.* **1994**, *45*, 685.
(25) *Chemical Reactions in Clusters*; Bernstein, E. R., Ed.; Oxford University Press: Oxford, 1996.
(26) Anderson, J. B.; Andres, R. P.; Fenn, J. B. *Adv. Chem. Phys.* **1966**, *10*, 275. Hagena, O. F. *Surf. Sci.* **1981**, *106*, 101.
(27) Zhong, Q.; Castleman, A. W., Jr. *Chem. Rev.* **2000**, *100*, 4039.
(28) *Femtochemistry-Ultrafast Dynamics of the Chemical Bond*; Zewail, A. H., Ed.; World Scientific (20th Century Chemistry Series): River Edge, NJ, Singapore, 1994.
(29) *Femtosecond Chemistry*; Manz, J., Woste, L., Eds.; VCH Verlagsellschaft: Weinheim, 1995.
(30) Zewail, A. H. *J. Phys. Chem.* **1996**, *100*, 12701.
(31) Dantus, M.; Rosker, M. J.; Zewail, A. H. *J. Chem. Phys.* **1987**, *87*, 2395.
(32) Zewail, A. H. *Science* **1988**, *242*, 1645.
(33) Huneycutt, A. J.; Saykally, R. J. *Science* **2003**, *299*, 1329.
(34) Robertson, W. H.; Johnson, M. A. *Science* **2002**, *298*, 69.
(35) Hurley, S. M.; Dermota, T. E.; Hydutsky, D. P.; Castleman, A. W., Jr. *J. Chem. Phys.* **2003**, *118*, 9272.
(36) Hurley, S. M.; Dermota, T. E.; Hydutsky, D. P.; Castleman, A. W., Jr. *Science* **2002**, *298*, 202.
(37) Hurley, S. M.; Zhong, Q.; Castleman, A. W., Jr. *J. Chem. Phys.* **2000**, *112*, 4644.
(38) Dedonder-Lardeux, C.; Gregoire, G.; Jouvet, C.; Martrenchard, S.; Solgadi, D. *Chem. Rev.* **2000**, *100*, 4023.
(39) Gregoire, G.; Mons, M.; Dimicoli, I.; Dedonder-Lardeux, C.; Jouvet, C.; Martrenchard, S.; Solgadi, D. *J. Chem. Phys.* **2000**, *112*, 8794.
(40) Gregoire, G.; Mons, M.; Dimicoli, I.; Dedonder-Lardeux, C.; Jouvet, C.; Martrenchard, S.; Solgadi, D. *J. Chem. Phys.* **1999**, *110*, 1521.
(41) Grosberg, A. Y.; Nguyen, T. T.; Shklovskii, B. I. *Rev. Mod. Phys.* **2002**, *74*, 329.
(42) Jortner, J.; Bixon, M.; Langenbacher, T.; Michel-Beyerle, M. E. *Proc. Natl. Acad. Sci. U.S.A.* **1998**, *95*, 12759.
(43) Stowell, M. H. B.; McPhillips, T. M.; Rees, D. C.; Soltis, S. M.; Abresch, E.; Feher, G. *Science* **1997**, *276*, 812.
(44) *Femtochemistry and Femtobiology*; Sundström, V., Ed.; Imperial College Press: London, 1996.
(45) Kelley, S. O.; Barton, J. K. *Science* **1999**, *283*, 375.
(46) Castleman, A. W., Jr.; Zhong, Q.; Hurley, S. M. *Proc. Natl. Acad. Sci.* **1999**, *96*, 4219.
(47) Kosower, E. M.; Huppert, D. *Annu. Rev. Phys. Chem.* **1986**, *37*, 127.
(48) Benesi, H. A.; Hildebrand, J. H. *J. Am. Chem. Soc.* **1949**, *71*, 2703.
(49) Mulliken, R. S. *J. Am. Chem. Soc.* **1950**, *72*, 600.
(50) Cheng, P. Y.; Zhong, D.; Zewail, A. H. *J. Chem. Phys.* **1996**, *105*, 6216.
(51) Zhong, D.; Zewail, A. H. *Proc. Natl. Acad. Sci.* **1999**, *96*, 2602.
(52) Su, J. T.; Zewail, A. H. *J. Phys. Chem. A* **1998**, *102*, 4082.
(53) DeBoer, G.; Young, M. A. *J. Chem. Phys.* **1997**, *106*, 5468.
(54) DeBoer, G.; Preszler-Prince, A.; Young, M. A. *J. Chem. Phys.* **2001**, *115*, 3112.
(55) Guidoni, A. G.; Paladini, A.; Veneziani, M.; Naaman, R.; Di Palma, T. M. *Appl. Surf. Sci.* **2000**, *154*, 186.
(56) Förster, T. *Z. Elektrochem.* **1950**, *54*, 531.
(57) Weller, A. *Z. Elektrochem.* **1952**, *56*, 662.
(58) Syage, J. A.; Steadman, J. *J. Chem. Phys.* **1991**, *95*, 2497.
(59) Kim, S. K.; Wang, J.-K.; Zewail, A. H. *Chem. Phys. Lett.* **1994**, *228*, 369.
(60) Syage, J. A. *J. Phys. Chem.* **1995**, *99*, 5772.
(61) Kim, S. K.; Breen, J. J.; Willberg, D. M.; Peng, L. W.; Heikal, A.; Sayage, J. A.; Zewail, A. H. *J. Phys. Chem.* **1995**, *99*, 7421.
(62) Knochenmuss, R. *Chem. Phys. Lett.* **1998**, *293*, 191.
(63) Knochenmuss, R. *Chem. Phys. Lett.* **1999**, *311*, 439.
(64) Lührs, D. C.; Knochenmuss, R.; Fischer, I. *Phys. Chem. Chem. Phys.* **2000**, *2*, 4335.
(65) Knochenmuss, R.; Holtom, G. R.; Ray, D. *Chem. Phys. Lett.* **1993**, *215*, 188.
(66) Knochenmuss, R.; Smith, D. E. *J. Chem. Phys.* **1994**, *101*, 7327.
(67) Steadman, J.; Syage, J. A. *J. Chem. Phys.* **1990**, *92*, 4630.
(68) Syage, J. A. In *Femtosecond Chemistry*; Manz, J., Wöste, L., Eds.; Springer-Verlag: Germany, 1994; p 475.
(69) Pino, G.; Grégoire, G.; Dedonder-Lardeux, C.; Jouvet, C.; Martrenchard, S.; Solgadi, D. *Phys. Chem. Chem. Phys.* **2000**, *2*, 893.
(70) Grégoire, G.; Dedonder-Lardeux, C.; Jouvet, C.; Martrenchard, S.; Peremans, A.; Solgadi, D. *J. Phys. Chem. A* **2000**, *104*, 9087.
(71) David, O.; Dedonder-Lardeux, C.; Jouvet, C. *Int. Rev. Phys. Chem.* **2002**, *21*, 499.
(72) Knochenmuss, R.; Fischer, I. *Int. J. Mass Spectrom.* **2002**, *220*, 343.
(73) Cheshnovsky, O.; Leutwyler, S. *J. Chem. Phys.* **1988**, *88*, 4127.
(74) Knochenmuss, R.; Fischer, I.; Lührs, D.; Lin, Q. *Isr. J. Chem.* **1999**, *39*, 221.
(75) Ishiuchi, S.; Saeki, M.; Sakai, M.; Fujii, M. *Chem. Phys. Lett.* **2000**, *322*, 27.
(76) Siebrand, W.; Zgierski, M. Z. *Chem. Phys. Lett.* **2000**, *320*, 153.
(77) Siebrand, W.; Zgierski, M. Z. *Chem. Phys. Lett.* **2001**, *334*, 127.
(78) Sobolewski A. L.; Domcke, W. *J. Phys. Chem. A* **2001**, *105*, 9275.
(79) Martrenchard-Barra, S.; Dedonder-Lardeux, C.; Jouvet, C.; Solgadi, D.; Vervloet, M.; Grégoire, G.; Dimicoli, I. *Chem. Phys. Lett.* **1999**, *310*, 173.
(80) Snyder, E. M.; Castleman, A. W., Jr. *J. Chem. Phys.* **1997**, *107*, 744.
(81) Wei, S.; Purnell, J.; Buzza, S. A.; Castleman, A. W., Jr. *J. Chem. Phys.* **1993**, *99*, 755.
(82) Farmanara, P.; Radloff, W.; Stert, V.; Ritze, H.-H.; Hertel, I. V. *J. Chem. Phys.* **1999**, *111*, 633.
(83) Farmanara, P.; Ritze, H.-H.; Stert, V.; Radloff, W.; Hertel, I. V. *Eur. Phys. J. D* **2002**, *19*, 193.
(84) Wisniewski, E. S.; Hershberger, M. A.; Castleman, A. W., Jr. *J. Chem. Phys.* **2002**, *116*, 5738.
(85) Lippert, H.; Stert, V.; Hesse, L.; Schulz, C. P.; Hertel, I. V.; Radloff, W. *Chem. Phys. Lett.* **2003**, *371*, 208.
(86) Lippert, H.; Stert, V.; Hesse, L.; Schulz, C. P.; Radloff, W.; Hertel, I. V. *Eur. Phys. J. D* **2002**, *20*, 445.
(87) Stert, V.; Hesse, L.; Lippert, H.; Schulz, C. P.; Radloff, W. *J. Phys. Chem. A* **2002**, *106*, 5051.
(88) *Lippert, H.; Stert, V.; Hesse, L.; Schulz, C. P.; Hertel, I. V.; and Radloff, W. J. Phys. Chem. A* **2003**, *107*, 8239.
(89) Lippert, H.; Stert, V.; Hesse, L.; Schulz, C. P.; Hertel, I. V.; Radloff, W. *Chem. Phys. Lett.* **2003**, *376*, 40.
(90) Watson, J. D. H.; Crick, F. H. C. *Nature* **1953**, *171*, 737.
(91) Goodman, M. F. *Nature* **1995**, *378*, 237.
(92) Folmer, D. E.; Poth, L.; Wisniewski, E. S.; Castleman, A. W., Jr. *Chem. Phys. Lett.* **1998**, *287*, 1.

(93) Folmer, D. E.; Wisniewski, E. S.; Castleman, A. W., Jr. *Chem. Phys. Lett.* **2000**, *318*, 637.
(94) Taylor, C. A.; El Bayoumi, M. A.; Kasha, M. *Proc. Natl. Acad. Sci.* **1969**, *63*, 253.
(95) Fuke, K.; Yoshiuchi, H.; Kaya, K. *J. Phys. Chem.* **1984**, *88*, 5840.
(96) Fuke, K.; Kaya, K. *J. Phys. Chem.* **1989**, *93*, 614.
(97) Nakajima, A.; Ono, F.; Kihara, Y.; Ogawa, A.; Matsurbara, K.; Ishikawa, K.; Baba, M.; Kaya, K. *Laser Chem.* **1995**, *15*, 167.
(98) Nakajima, A.; Hirano, M.; Hasumi, R.; Kaya, K.; Watanabe, H.; Carter, C. C.; Williamson, J. M.; Miller, T. *J. Phys. Chem.* **1997**, *101*, 392.
(99) Douhal, A.; Kim, S. K.; Zewail, A. H. *Nature* **1995**, *378*, 260.
(100) Guallar, V.; Batista, V. S.; Miller, W. H. *J. Chem. Phys.* **1999**, *110*, 9922.
(101) Chou, P. T.; Wu, G. R.; Wei, C. Y.; Cheng, C. C.; Chang, C. P.; Hung, F. T. *J. Phys. Chem. B* **2000**, *104*, 7818.
(102) Chou, P. T.; Wu, G. R.; Wei, C. Y.; Shiao, M. Y.; Liu, Y. I. *J. Phys. Chem. A* **2000**, *104*, 8863.
(103) Folmer, D. E.; Wisniewski, E. S.; Hurley, S. M.; Castleman, A. W., Jr. *Proc. Natl. Acad. Sci.* **1999**, *96*, 12980.
(104) Hobza, P. Personal communication.
(105) Ishikawa, H.; Iwata, K.; Hamaguchi, H. *J. Phys. Chem. A* **2002**, *106*, 2305.
(106) Podolyan, Y.; Gorb, L.; Leszczynski, J. *J. Phys. Chem. A* **2002**, *106*, 12103. Dziekonski, P.; Sokalski, W. A.; Podolyan, Y.; Leszczynski, J. *Chem. Phys. Lett.* **2003**, *367*, 367.
(107) El-Kemary, M. A.; El-Gezawy, H. S.; El-Baradie, H. Y.; Issa, R. M. *Chem. Phys.* **2001**, *265*, 233.
(108) Farmanara, P.; Stert, V.; Radloff, W.; Hertel, I. V. *J. Phys. Chem. A* **2001**, *105*, 5613.
(109) Radloff, W.; Stert, V.; Freudenberg, T.; Hertel, I. V.; Jouvet, C.; Dedonder-Lardeux, C.; Solgadi, D. *Chem. Phys. Lett.* **1997**, *281*, 20.
(110) Radloff, W.; Freudenberg, T.; Ritze, H. H.; Stert, V.; Noack, F.; Hertel, I. V. *Chem. Phys. Lett.* **1996**, *261*, 301.
(111) Radloff, W.; Freudenberg, T.; Stert, V.; Ritze, H. H.; Noack, F.; Hertel, I. V. *Chem. Phys. Lett.* **1997**, *264*, 210.
(112) Radloff, W.; Freudenberg, T.; Ritze, H. H.; Stert, V.; Weyers, K.; Noack, F. *Chem. Phys. Lett.* **1995**, *245*, 400.
(113) Stert, V.; Radloff, W.; Schulz, C. P.; Hertel, I. V. *Eur. Phys. J. D* **1999**, *5*, 97.
(114) de Vivie-Riedle, R.; Schulz, S.; Hohndorf, J.; Schulz, C. P. *Chem. Phys.* **1997**, *225*, 299.
(115) Schulz, C. P.; Hohndorf, J.; Brockhaus, P.; Hertel, I. V. *Z. Phys. D* **1997**, *40*, 78.
(116) Schulz, C. P.; Hohndorf, J.; Brockhaus, P.; Noack, F.; Hertel, I. V. *Chem. Phys. Lett.* **1995**, *239*, 18.
(117) Schulz, C. P.; Scholz, A.; Hertel, I. V. *Ultrafast reaction in solvated metal atom clusters: A dynamics study in the visible and near-IR spectral range*; Elsässer, T., Fujimoto, F., Wiersma, D. A., Zinth W., Eds.; *Ultrafast Phenomena XI*; Springer-Verlag: Berlin, 1998; 621.
(118) Stert, V.; Hesse, L.; Schulz, C. P.; Radloff, W. *Chem. Phys. Lett.* **2001**, *341*, 501.
(119) Poth, L.; Zhong, Q.; Ford, J. V.; Castleman, A. W., Jr. *J. Chem. Phys.* **1998**, *109*, 4791.
(120) Hurley, S. M.; Dermota, T. E.; Hydutsky, D. P.; Castleman, A. W., Jr. *Int. J. Mass. Spectrom.* **2003**, *228*, 677.
(121) Donaldson, D. J.; Child, M. S.; Vaida, V. *J. Chem. Phys.* **1988**, *88*, 7410.
(122) Guo, H.; Zewail, A. H. *Can. J. Chem.* **1994**, *72*, 947.
(123) Janssen, M. H. M.; Dantus, M.; Guo, H.; Zewail, A. H. *Chem. Phys. Lett.* **1993**, *214*, 281.
(124) Donaldson, D. J.; Vaida, V.; Naaman, R. *J. Chem. Phys.* **1987**, *87*, 2522.
(125) ter Steege, D. H. A.; Wirtz, A. C.; Buma, W. J. *J. Chem. Phys.* **2002**, *116*, 547.
(126) Donaldson, D. J.; Gaines, G. A.; Vaida V. *J. Phys. Chem.* **1988**, *92*, 2766.
(127) Vaida, V.; Donaldson, D. J.; Sapers, S. P.; Naaman, R.; Child, M. S. *J. Phys. Chem.* **1989**, *93*, 513.
(128) Hurley, S. M.; Dermota, T. E.; Hydutsky, D. P.; Castleman, A. W., Jr. *J. Phys. Chem. A* **2003**, *107*, 3497.
(129) Sorgues, S.; Mestdagh, J.-M.; Gloaguen, E.; Visticot, J.-P.; Heninger, M.; Mestdagh, H.; Soep, B. Submitted for publication.
(130) Liu, Q. L.; Wang, J. K.; Zewail, A. H. *Nature* **1993**, *364*, 427.
(131) Potter, E. D.; Liu, Q.; Zewail, A. H. *Chem. Phys. Lett.* **1992**, *200*, 605.
(132) Wang, J. K.; Liu, Q. L.; Zewail, A. H. *J. Phys. Chem.* **1995**, *99*, 11309.
(133) Liu Q. L.; Wang, J. K.; Zewail, A. H. J. *Phys. Chem.* **1995**, *99*, 11321.
(134) Cheng, P. Y.; Zhong, D.; Zewail, A. H. *Chem. Phys. Lett.* **1995**, *237*, 399.
(135) Cheng, P. Y.; Zhong, D.; Zewail, A. H. *J. Phys. Chem.* **1995**, *99*, 15733.
(136) Zhong; D.; Cheng, P. Y.; Zewail, A. H. *J. Chem. Phys.* **1996**, *105*, 7864.
(137) Vorsa, V.; Nandi, S.; Campagnola, P. J.; Larsson, M.; Lineberger, W. C. *J. Chem. Phys.* **1997**, *106*, 1402.
(138) Papanikolas, J. M.; Vorsa, V.; Nadal, M. E.; Campagnola, P. J.; Buchenau, H. K.; Lineberger, W. C. *J. Chem. Phys.* **1993**, *99*, 8733.
(139) Sanov, A.; Sanford, T.; Nandi, S.; Lineberger, W. C. *J. Chem. Phys.* **1999**, *111*, 664.
(140) Sanov, A.; Nandi, S.; Lineberger, W. C. *J. Chem. Phys.* **1998**, *108*, 5155.
(141) Greenblatt, B. J.; Zanni, M. T.; Neumark, D. M. *Science* **1997**, *276*, 1675.
(142) Greenblatt, B. J.; Zanni, M. T.; Neumark, D. M. *J. Chem. Phys.* **1999**, *111*, 10566.
(143) Greenblatt, B. J.; Zanni, M. T.; Neumark, D. M. *J. Chem. Phys.* **2000**, *112*, 601.
(144) Sanov, A.; Lineberger, W. C. *PhysChemComm* **2002**, *5*, 165.
(145) Paik, D. H.; Bernhardt, T. M.; Kim, N. J.; Zewail A. H. *J. Chem. Phys.* **2001**, *115*, 612.
(146) Kim, N. J.; Paik, D. H.; Zewail A. H. *J. Chem. Phys.* **2003**, *118*, 6930.
(147) Pontius, N.; Bechthold, P. S.; Neeb, M.; Eberhardt, W. *J. Electron Spectrosc. Relat. Phenom.* **2001**, *114*, 163.
(148) Pontius, N.; Luttgens, G.; Bechthold, P. S.; Neeb, M.; Eberhardt, W. *J. Chem. Phys.* **2001**, *115*, 10479.
(149) Pontius, N.; Bechthold, P. S.; Neeb, M.; Eberhardt, W. *Phys. Rev. Lett.* **2000**, *84*, 1132.
(150) Pontius, N.; Neeb, M.; Eberhardt, W.; Luttgens, G.; Bechthold, P. S. *Phys. Rev. B* **2003**, *67*, 035425.
(151) Pontius, N.; Bechthold, P. S.; Neeb, M.; Eberhardt, W. *Appl. Phys. B* **2000**, *71*, 351.
(152) Luttgens, G.; Pontius, N.; Bechthold, P. S.; Neeb, M.; Eberhardt, W. *Phys. Rev. Lett.* **2002**, *88*, 076102.
(153) Gantefor, G.; Kraus, S.; Eberhardt, W. *J. Electron Spectrosc.* **1998**, *88*, 35.
(154) Wolf, S.; Sommerer, G.; Rutz, S.; Schreiber, E.; Leisner, T.; Woste, L. *Phys. Rev. Lett.* **1995**, *74*, 4177.
(155) Leisner, T.; Vajda, S.; Wolf, S.; Woste, L.; Berry, R. S. *J. Chem. Phys.* **1999**, *111*, 1017.
(156) Hess, H.; Kwiet, S.; Socaciu, L.; Wolf, S.; Leisner, T.; Woste, L. *Appl. Phys. B* **2000**, *71*, 337.
(157) Hartmann, M.; Pittner, J.; Bonacic-Koutecky, V.; Heidenreich, A.; Jortner, J. *J. Chem. Phys.* **1998**, *108*, 3096.
(158) Jeschke, H. O.; Garcia, M. E.; Bennemann, K. H. *Phys. Rev. A* **1996**, *54*, R4601.
(159) Hess, H.; Asmis, K. R.; Leisner, T.; Woste, L. *Eur. Phys. J. D* **2001**, *16*, 145.
(160) Boo, D. W.; Ozaki, Y.; Andersen L. H.; Lineberger, W. C. *J. Phys. Chem. A* **1997**, *101*, 6688.
(161) Berry, R. S.; Bonacic-Koutecky, V.; Gaus, J.; Leisner, T.; Manz, J.; Reischl-Lenz, B.; Ruppe, H.; Rutz, S.; Schreiber, E.; Vajda, S.; de Vivie-Riedle, R.; Wolf, S.; Woste, L.; Gerber, G.; Letokhov, V. S.; Rice, S. A.; Zewail, A. H.; Marcus, R. A.; Tannor, D. J.; Kobayashi, T. *Chemical Reactions and Their Control on the Femtosecond Time Scale, XXth Solvay Conference on Chemistry* 1997, Vol. 101, p 101.
(162) Woste, L. *Z. Phys. D* **1996**, *196*, 1.
(163) Assion, A.; Baumert, T.; Helbing, J.; Seyfried, V.; Gerber, G. *Phys. Rev. A* **1997**, *55*, 1899.
(164) Assion, A.; Baumert, T.; Seyfried, V.; Weiss, V.; Wiedenmann, E.; Gerber, G. *Z. Phys. D* **1996**, *36*, 265.
(165) Baumert, T.; Gerber, G. *Isr. J. Chem.* **1994**, *34*, 103.
(166) Engel, V.; Baumert, T.; Meier, C.; Gerber, G. *Z. Phys. D* **1993**, *28*, 37.
(167) Baumert, T.; Thalweiser, R.; Weiss, V.; Gerber, G. *Z. Phys. D* **1993**, *26*, 131.
(168) Baumert, T.; Engel, V.; Meier, C.; Gerber, G. *Chem. Phys. Lett.* **1992**, *200*, 488.
(169) Baumert, T.; Rottgermann, C.; Rothenfusser, C.; Thalweiser, R.; Weiss, V.; Gerber, G. *Phys. Rev. Lett.* **1992**, *69*, 1512.
(170) Baumert, T.; Engel, V.; Rottgermann, C.; Strunz, W. T.; Gerber, G. *Chem. Phys. Lett.* **1992**, *191*, 639.
(171) Baumert, T.; Grosser M.; Thalweiser, R.; Gerber, G. *Phys. Rev. Lett.* **1991**, *67*, 3753.
(172) Kobe, K.; Kuhling, H.; Rutz, S.; Schreiber, E.; Wolf, J. P.; Woste, L.; Broyer, M.; Dugourd, P. *Chem. Phys. Lett.* **1993**, *213*, 554.
(173) Rutz, S.; Greschik, S.; Schreiber, E.; Woste, L. *Chem. Phys. Lett.* **1996**, *257*, 365.
(174) Kuhling, H.; Kobe, K.; Rutz, S.; Schreiber, E.; Woste, L. *J. Phys. Chem.* **1994**, *98*, 6679.
(175) Kuhling, H.; Rutz, S.; Kobe, K.; Schreiber, E.; Woste, L. *J. Phys. Chem.* **1993**, *97*, 12500.
(176) Gaus, J.; Kobe, K.; Bonacickoutecky, V.; Kuhling, H.; Manz, J.; Reischl, B.; Rutz, S.; Schreiber, E.; Woste, L. *J. Phys. Chem.* **1993**, *97*, 12509.
(177) Reischl, B.; de Vivie-Riedle, R.; Rutz, S.; Schreiber, E. *J. Chem. Phys.* **1996**, *104*, 8857.
(178) Rutz, S.; Ruppe, H.; Schreiber, E.; Woste, L. *Z. Phys. D* **1997**, *40*, 25.

(179) de Vivie-Riedle, R.; Kobe, K.; Manz, J.; Meyer, W.; Reischl, B.; Rutz, S.; Schreiber, E.; Woste, L. *J. Phys. Chem.* **1996**, *100*, 7789.
(180) Rutz, S.; Schreiber, E.; Woste, L. *Surf. Rev. Lett.* **1996**, *3*, 475.
(181) Ruppe, H.; Rutz, S.; Schreiber, E.; Woste, L. *Chem. Phys. Lett.* **1996**, *257*, 356.
(182) Ruff, A.; Rutz, S.; Schreiber, E.; Woste, L. *Z. Phys. D* **1996**, *37*, 175.
(183) Nicole, C.; Bouchene, M. A.; Meier, C.; Magnier, S.; Schreiber, E.; Girard, B. *J. Chem. Phys.* **1999**, *111*, 7857.
(184) Heufelder, J.; Ruppe, H.; Rutz, S.; Schreiber, E.; Woste, L. *Chem. Phys. Lett.* **1997**, *269*, 1.
(185) Guo, B. C.; Kerns, K. P.; Castleman, A. W., Jr. *Science* **1992**, *255*, 1411.
(186) Wei, S.; Guo, B. C.; Purnell, J.; Buzza, S. A.; Castleman, A. W., Jr. *J. Phys. Chem.* **1994**, *98*, 9682.
(187) Wei, S.; Guo, B. C.; Purnell, J.; Buzza, S. A.; Castleman, A. W., Jr. *J. Phys. Chem.* **1992**, *96*, 4166.
(188) Wei, S.; Guo, B. C.; Purnell, J.; Buzza, S. A.; Castleman, A. W., Jr. *Science* **1992**, *256*, 818.
(189) Pilgrim, J. S.; Duncan, M. A. *J. Am. Chem. Soc.* **1993**, *115*, 6958.
(190) Guo, B. C.; Castleman, A. W., Jr. In *Advances in Metal and Semiconductor Clusters*; Duncan, M., Ed.; JAI Press: 1994; Vol. 2, p 137.
(191) Cartier, S. F.; May, B. D.; Castleman, A. W., Jr. *J. Chem. Phys.* **1994**, *100*, 5384.
(192) Cartier, S. F.; May, B. D.; Castleman, A. W., Jr. *J. Am. Chem. Soc.* **1994**, *116*, 5295.
(193) Deng, H. T.; Guo, B. C.; Kerns, K. P.; Castleman, A. W., Jr. *Int. J. Mass Spectrom. Ion Processes* **1994**, *138*, 275.
(194) Guo, B. C.; Kerns, K. P.; Castleman, A. W., Jr. *J. Am. Chem. Soc.* **1993**, *115*, 7415.
(195) Wei, S.; Guo, B. C.; Purnell, J.; Buzza, S. A.; Castleman, A. W., Jr. *J. Phys. Chem.* **1993**, *97*, 9559.
(196) Cartier, S. F.; May, B. D.; Toleno, B. J.; Purnell, J.; Wei, S.; Castleman, A. W., Jr. *Chem. Phys. Lett.* **1994**, *220*, 23.
(197) Wei, S.; Guo, B. C.; Deng, H. T.; Kerns, K.; Purnell, J.; Buzza, S. A.; Castleman, A. W., Jr. *J. Am. Chem. Soc.* **1994**, *116*, 4475.
(198) Wei, S.; Castleman, A. W., Jr. *Chem. Phys. Lett.* **1994**, *227*, 305.
(199) Purnell, J.; Wei, S.; Castleman, A. W., Jr. *Chem. Phys. Lett.* **1994**, *229*, 105.
(200) Kerns, K. P.; Guo, B. C.; Deng, H. T.; Castleman, A. W., Jr. *J. Am. Chem. Soc.* **1995**, *117*, 4026.
(201) Deng, H. T.; Guo, B. C.; Kerns, K. P.; Castleman, A. W., Jr. *J. Phys. Chem.* **1994**, *98*, 13373.
(202) Kerns, K. P.; Guo, B. C.; Deng, H. T.; Castleman, A. W., Jr. *J. Chem. Phys.* **1994**, *101*, 8529.
(203) Deng, H. T.; Kerns, K. P.; Castleman, A. W., Jr. *J. Am. Chem. Soc.* **1996**, *118*, 446.
(204) Cartier, S. F.; May, B. D.; Castleman, A. W., Jr. *J. Phys. Chem.* **1996**, *100*, 8175.
(205) Lee, S.; Gotts, N. G.; von Helden, G.; Bowers, M. T. *Science* **1995**, *267*, 999.
(206) Yeh, C. S.; Afzaal, S.; Lee, S. A.; Byun, Y. G.; Freiser, B. S. *J. Am. Chem. Soc.* **1994**, *116*, 8806.
(207) Grimes, R. W.; Gale, J. D. *J. Chem. Soc., Chem. Commun.* **1992**, *17*, 1222.
(208) Reddy, B. V.; Khanna, S. N.; Jena, P. *Science* **1992**, *258*, 1640.
(209) Rantala, T.; Jelski, D. A.; Bowser, J. R.; Xia, X.; George, T. F. *Z. Phys. D* **1993**, *26*, S255.
(210) (a) Methfessel, M.; van Schilfgaarde, M.; Scheffler, M. *Phys. Rev. Lett.* **1993**, *70*, 29. (b) *Phys. Rev. Lett.* **1993**, *71*, 209.
(211) Grimes, R. W.; Gale, J. D. *J. Phys. Chem.* **1993**, *97*, 4616.
(212) Ceulemans, A.; Fowler, P. W. *J. Chem. Soc., Faraday Trans.* **1992**, *88*, 2797.
(213) Rohmer, M. M.; De Vaal, P.; Bénard, M. *J. Am. Chem. Soc.* **1992**, *114*, 9696.
(214) Lin, Z. Y.; Hall, M. B. *J. Am. Chem. Soc.* **1992**, *114*, 10054.
(215) Dance, I. *J. Chem. Soc., Chem. Commun.* **1992**, *24*, 1779.
(216) Chen, H.; Feyereisen, M.; Long, X. P.; Fitzgerald, G. *Phys. Rev. Lett.* **1993**, *71*, 1732.
(217) Rohmer, M.-M.; Bénard, M.; Henrite, C.; Bo, C.; Poblet, J.-M. *J. Chem. Soc., Chem. Commun.* **1993**, *15*, 1182.
(218) Pauling, L. *Proc. Natl. Acad. Sci. U.S.A.* **1992**, *89*, 8175.
(219) Dance, I. G. *Aust. J. Chem.* **1993**, *46*, 727.
(220) Rohmer, M.-M.; Bénard, M.; Bo, C.; Poblet, J.-M. *J. Am. Chem. Soc.* **1995**, *117*, 508.
(221) Khan, A. *J. Phys. Chem.* **1995**, *99*, 4923.
(222) Cartier, S. F.; Chen, Z. Y.; Walder, G. J.; Sleppy, C. R.; Castleman, A. W., Jr. *Science* **1993**, *260*, 195.
(223) May, B. D.; Cartier, S. F.; Castleman, A. W., Jr. *Chem. Phys. Lett.* **1995**, *242*, 265.
(224) Cartier, S. F.; May, B. D.; Castleman, A. W., Jr. *J. Chem. Phys.* **1996**, *104*, 3423.
(225) Kooi, S. E.; Castleman, A. W., Jr. *J. Chem. Phys.* **1998**, *108*, 8864.
(226) Kooi, S. E.; Leskiw, B. D.; Castleman, A. W., Jr. *Nano Lett.* **2001**, *1*, 113.
(227) Leskiw, B. D.; Knappenberger, K. L.; Castleman, A. W., Jr. *J. Chem. Phys.* **2002**, *117*, 8321.
(228) Wisniewski, E. S.; Leskiw, B. D.; Hurley, S. M.; Dermota, T. E.; Hydutsky, D. P.; Knappenberger, K. L., Jr.; Hershberger, M.; Castleman, A. W., Jr. World Scientific: River Edge, NJ, 2001.
(229) Sakurai, H.; Kooi, S. E.; Castleman, A. W., Jr. *J. Cluster Sci.* **1999**, *10*, 493.
(230) Sakurai, H.; Castleman, A. W., Jr. *J. Phys. Chem. A* **1997**, *101*, 7695.
(231) Sakurai, H.; Castleman, A. W., Jr. *J. Phys. Chem. A* **1998**, *102*, 10486.
(232) Jena, P.; Khanna, S. N.; Rao, B. K. In *Clusters and Fullerenes*; Kumar, V., Martin, T. P., Tosatti, E., Eds.; World Scientific: River Edge, NJ, 1992; p 73.
(233) Reddy, B. V.; Khanna, S. N. *Chem. Phys. Lett.* **1993**, *209*, 104.
(234) Li, Z.-Q.; Gu, B.-L.; Han, R.-S.; Zheng, Q.-Q. *Z. Phys. D* **1993**, *27*, 275.
(235) Lou, L.; Guo, T.; Nordlander, P.; Smalley, R. E. *J. Chem. Phys.* **1993**, *99*, 5301.
(236) Khan, A. *J. Phys. Chem.* **1993**, *97*, 10937.
(237) Rohmer, M.-M.; Bénard, M.; Poblet, J.-M. *Chem. Rev.* **2000**, *100*, 495. Hou, H.; Muckerman, J. T.; Liu. P.; Rodriguez, J. A. *J. Phys. Chem. A* **2003**, *107*, 9344.
(238) Leisner, T.; Athanassenas, K.; Kreisle, D.; Rechnagel, E.; Echt, O. *J. Chem. Phys.* **1993**, *99*, 9670.
(239) Leisner, T.; Athanassenas, K.; Echt, O.; Kandler, O.; Kreisle, D.; Rechnagel, E. *Z. Phys. D* **1991**, *20*, 127.
(240) Collings, B. A.; Amrein, A. H.; Rayner, D. M.; Hackett, P. A. *J. Chem. Phys.* **1993**, *99*, 4174.
(241) Nieman, G. C.; Parks, E. K.; Richtsmeier, S. C.; Liu, K.; Pobo, L. G.; Riley, S. J. *High Temp. Sci.* **1986**, *22*, 115.
(242) Athanassenas, K.; Leisner, T.; Frenzel, U.; Kreisle, D. *Ber. Bunsen-Ges. Phys. Chem.* **1992**, *96*, 1192.
(243) Amrein, A.; Simpson, R.; Hackett, P. *J. Chem. Phys.* **1991**, *95*, 1781.
(244) Stairs, J. R.; Davis, K. M.; Peppernick S. J.; Castleman, A. W., Jr. *J. Chem. Phys.* **2003**, *119*, 7857. Stairs, J. R.; Castleman, A. W., Jr. *Int. J. Mass Spectrom.* **2002**, *216*, 75.
(245) Campbell, E. E. B.; Ulmer, G.; Hertel, I. V. *Phys. Rev. Lett.* **1991**, *67*, 1986.
(246) Ding, D.; Huang, J.; Compton, R. N.; Klots, C. E.; Haufler, R. E. *Phys. Rev. Lett.* **1994**, *73*, 1084.
(247) Campbell, E. E. B.; Hoffmann, K.; Hertel, I. V. *Eur. Phys. J. D* **2001**, *16*, 345.
(248) Lin, H.; Han, K.-L.; Bao, Y.; Gallogly, E. B.; Jackson, W. M. *J. Phys. Chem.* **1994**, *98*, 12495.
(249) Klots, C. E. *Chem. Phys. Lett.* **1991**, *186*, 73.
(250) Voisin, C.; Del Fatti, N.; Christofilos, D.; Vallée, F. *J. Phys. Chem. B* **2001**, *105*, 2264.
(251) Kreisle, D.; Echt, O.; Knapp, M.; Recknagel, E.; Leiter, K.; Mark, T. D.; Saenz, J. J.; Soler, J. M. *Phys. Rev. Lett.* **1986**, *56*, 1551.
(252) Brechignac, C.; Cahuzae, P.; Carlier, F.; de Frutos, M.; Barnett, R. N.; Landman, U. *Phys. Rev. Lett.* **1994**, *72*, 1636.
(253) Shukla, A. K.; Moore, C.; Stace, A. J. *Chem. Phys. Lett.* **1984**, *109*, 324. Stace, A. J. *Phys. Rev. Lett.* **1988**, *61*, 306.
(254) Kreisle, D.; Leiter, K.; Echt, O.; Mark, T. D. *Z. Phys. D* **1986**, *3*, 319.
(255) Scheier, P.; Mark, T. D. *J. Chem. Phys.* **1987**, *86*, 3056.
(256) Lezius, M.; Mark, T. D. *Chem. Phys. Lett.* **1989**, *155*, 496.
(257) Scheier, P.; Stamatovic, A.; Mark, T. D. *J. Chem. Phys.* **1988**, *88*, 4289.
(258) Scheier, P.; Dunser, B.; Mark, T. D. *Phys. Rev. Lett.* **1995**, *74*, 3368.
(259) Codling, K.; Frasinski, L. J.; Hatherly, P.; Barr, J. R. M. *J. Phys. B* **1987**, *20*, L525.
(260) Frasinski, L. J.; Codling, K.; Hatherly, P.; Barr, J.; Ross, I. N.; Toner, W. T. *Phys. Rev. Lett.* **1987**, *58*, 2424.
(261) Frasinski, L. J.; Codling, K.; Hatherly, P. A. *Science* **1989**, *246*, 1029.
(262) Lompre, L. A.; Mainfray, G. In *Multiphoton Processes*; Lambropoulos, P., Smith, S. J., Eds.; Springer-Verlag: Berlin, 1984; p 23.
(263) Johann, U.; Luk, T. S.; McIntyre, I. A.; McPherson, A.; Schwarzenbach, A. P.; Boyer, K.; Rhodes, C. K. *Multiphoton Ionization in Intense Ultraviolet Laser Fields (Proceedings of the Topical Meeting on Short Wavelength Coherent Generation)*; Attwood, D. T., Bokor, J., Eds.; AIP Conference Proceedings No. 147; AIP: New York, 1986; p 157.
(264) l'Huillier, A.; Lompre, L. A.; Mainfray, G.; Manus, C. *Phys. Rev. A* **1983**, *27*, 2503.
(265) Luk, T. S.; Johann, U.; Egger, H.; Pummer, H.; Rhodes, C. K. *Phys. Rev. A* **1985**, *32*, 214.
(266) Boyer, K.; Luk, T. S.; Solem, J. C.; Rhodes, C. K. *Phys. Rev. A* **1989**, *39*, 1186.
(267) Cornaggia, C.; Lavancier, J.; Normand, D.; Morellec, J.; Liu, H. X. *Phys. Rev. A* **1990**, *42*, 5464.
(268) Codling, K.; Frasinski, L. J.; Hatherly, P. A. *J. Phys. B* **1988**, *21*, L433.
(269) Hatherly, P. A.; Frasinski, L. J.; Codling, K.; Langley, A. J.; Shaikh, W. *J. Phys. B* **1990**, *23*, L291.

(270) Lavancier, J.; Normand, D.; Cornaggia, C.; Morellec, J.; Liu, H. X. *Phys. Rev. A* **1991**, *43*, 1461.
(271) Normand, D.; Cornaggia, C.; Lavancier, J.; Morellec, J.; Liu, H. X. *Phys. Rev. A* **1991**, *44*, 475.
(272) Snyder, E. M.; Wei, S.; Purnell, J.; Buzza, S. A.; Castleman, A. W., Jr. *Chem. Phys. Lett.* **1996**, *248*, 1.
(273) Purnell, J.; Snyder, E. M.; Wei, S.; Castleman, A. W., Jr. *Chem. Phys. Lett.* **1994**, *229*, 333.
(274) Snyder, E. M.; Buzza, S. A.; Castleman, A. W., Jr. *Phys. Rev. Lett.* **1996**, *77*, 3347.
(275) Ditmire, T.; Zweiback, J.; Yanovsky, V. P.; Cowan, T. E.; Hays, G.; Wharton, K. B. *Nature* **1999**, *398*, 489.
(276) Ditmire, T.; Springate, E.; Tisch, J. W. G.; Shao, Y. L.; Mason, M. B.; Hay, N.; Marangos, J. P.; Hutchinson, M. H. R. *Phys. Rev. A* **1998**, *57*, 369.
(277) Ditmire, T.; Tisch, J. W. G.; Springate, E.; Mason, M. B.; Hay, N.; Smith, R. A.; Marangos, J. P.; Hutchinson, M. H. R. *Nature* **1997**, *386*, 54.
(278) Ford, J. V.; Zhong, Q.; Poth, L.; Castleman, A. W., Jr. *J. Chem. Phys.* **1999**, *110*, 6257.
(279) Ford, J. V.; Poth, L.; Zhong, Q.; Castleman, A. W., Jr. *Int. J. Mass Spectrom. Ion Processes* **1999**, *192*, 327.
(280) Rose-Petruck, C.; Schafer, K. J.; Barty, C. P. J. In *Application of Laser Plasma Radiation II*; Richardson, M. C., Kyrala, G. A, Eds.; SPIE: Bellingham, 1995; 2523, 272.
(281) Rose-Petruck, C.; Schafer, K. J.; Wilson, K. R.; Barty, C. P. J. *Phys. Rev. A* **1997**, *55*, 1182.
(282) McPherson, A.; Luk, T. S.; Thompson, B. D.; Boyer, K.; Rhodes, C. K. *Appl. Phys. B* **1993**, *57*, 337.
(283) McPherson, A.; Luk, T. S.; Thompson, B. D.; Borisov, A. B.; Shiryaev, O. B.; Chen, X.; Boyer, K.; Rhodes, C. K. *Phys. Rev. Lett.* **1994**, *72*, 1810.
(284) McPherson, A.; Thompson, B. D.; Borisov, A. B.; Boyer, K.; Rhodes, C. K *Nature* **1994**, *370*, 631.
(285) Boyer, K.; Thompson, B. D.; McPherson, A.; Rhodes, C. K. *J. Phys. B: At. Mol. Opt. Phys.* **1994**, *27*, 4373.
(286) Seideman, T.; Ivanov, M. Y.; Corkum, P. B. *Phys. Rev. Lett* **1995**, *75*, 2819.
(287) Constant, E.; Stapelfeldt, H.; Corkum, P. B. *Phys. Rev. Lett.* **1996**, *76*, 4140.
(288) Chelkowski, S.; Conjusteau, A.; Zuo, T.; Bandrauk, A. D. *Phys. Rev. A* **1996**, *54*, 3235.
(289) Chelkowski, S.; Bandrauk, A. D. *J. Phys. B: At. Mol. Opt. Phys.* **1995**, *28*, L723.
(290) Yu, H. T.; Bandrauk, A. D. *Phys. Rev. A* **1997**, *56*, 685.
(291) Yu, H. T.; Zuo, T.; Bandrauk, A. D. *J. Phys. B: At. Mol. Opt. Phys.* **1998**, *31*, 1533.
(292) Zuo, T.; Bandrauk, A. D. *Phys. Rev. A* **1995**, *52*, R2511.
(293) Zuo, T.; Bandrauk, A. D. *Phys. Rev. A* **1995**, *51*, R26.
(294) Last, I.; Schek, I.; Jortner, J. *J. Chem. Phys.* **1997**, *107*, 6685.
(295) Last, I.; Jortner, J. *Phys. Rev. A* **1998**, *58*, 3826.
(296) Last, I.; Jortner, J. *Phys. Rev. A* **2000**, *62*, 013201.
(297) Card, D. A.; Folmer, D. E.; Sato, S.; Buzza, S. A.; Castleman, A. W., Jr. *J. Phys. Chem. A* **1997**, *101*, 3417.
(298) Zuo, T.; Chelkowski, S.; Bandrauk, A. D. *Phys. Rev. A* **1993**, *48*, 3837.
(299) Chelkowski, S.; Zuo, T.; Atabek, O.; Bandrauk, A. D. *Phys. Rev. A* **1995**, *52*, 2977.
(300) Zuo, T.; Chelkowski, S.; Bandrauk, A. D. *Phys. Rev. A* **1994**, *49*, 3943.
(301) Stapelfeldt, H.; Constant, E.; Corkum, P. B. *Phys. Rev. Lett.* **1995**, *74*, 3780.
(302) Poth, L.; Castleman, A. W., Jr. *J. Phys. Chem A* **1998**, *102*, 4075.
(303) Levis, R. J.; Rabitz, H. A. *J. Phys. Chem. A* **2002**, *106*, 6427.
(304) Levis, R. J.; Menkir, G. M.; Rabitz, H. *Science* **2001**, *292*, 709.
(305) Wisniewski, E. S.; Stairs, J. R.; Castleman, A. W., Jr. *Int. J. Mass Spectrom.* **2001**, *212*, 273.
(306) McPherson, A.; Boyer, K.; Rhodes, C. K. *J. Phys. B: At. Mol. Opt.* **1994**, *27*, L637.
(307) Wei, S.; Purnell, J.; Buzza, S. A.; Snyder, E. M.; Castleman, A. W., Jr. In *Femtosecond Chemistry*; Manz, J., Wöste, L., Eds.; Springer-Verlag: Germany, 1994; pp 449.

CR020665E